The potential of portable luminescence readers in geomorphological investigations: a review

Ken Munyikwa[1], Tim C. Kinnaird[2], and David C.W. Sanderson[3]

[1]Centre for Science, Athabasca University, Athabasca, Alberta, Canada

[2]School of Earth and Environmental Sciences, University of St Andrews, St Andrews, Scotland, U.K.

[3]Scottish Universities Environmental Research Centre, East Kilbride, Glasgow, Scotland, U.K.

Correspondence

Ken Munyikwa, Centre for Science, Athabasca University, 1 University Drive, Athabasca, AB T9S 3A3, Canada,

kenm@athabascau.ca

ABSTRACT

The development of functional portable optically stimulated luminescence (OSL) readers over the last decade has provided practitioners with the capability to acquire luminescence signals from geological materials relatively rapidly, which allows for expedient preliminary chronostratigraphic insight when working with complex depositional systems of late Quaternary age. Typically, when using the portable OSL reader, infrared (IR) or blue post-IR OSL signals are acquired from bulk unprocessed materials, in contrast to regular luminescence dating which is usually based on measurements on pure

quartz or feldspar mineral separates, or on select silt-sized polymineralic portions. To demonstrate the utility of portable OSL measurements, this paper outlines the basic features of portable OSL readers and their constraints. Afterwards, case studies in which the instrument has been used to elucidate cryptostratigraphic variations in sedimentary sequences for geomorphological applications are reviewed. The studies can generally be grouped into three main categories. The first includes studies where the variation of portable OSL reader luminescence signal intensities with depth are plotted to generate profiles that contextualise sediment stratigraphy. In the second group, portable OSL reader luminescence signal intensities are used to interpret sediment processes that shed light on depositional histories. In the last category, luminescence signals from the portable OSL reader are calibrated to approximate numerical burial ages of depositional units. The paper concludes with a discussion of possible future directions.

Keywords geomorphology, dating, landscape evolution, optically stimulated luminescence, portable OSL reader, chronology

1. INTRODUCTION

Luminescence dating is an effective dating approach in the quantitative study of late Quaternary clastic depositional systems (e.g. Aitken, 1998; Wintle, 2008; Rhodes, 2011). Absolute ages acquired using the method help assign temporal frameworks to geomorphic events and environmental processes. The dating method is based on the ability of some minerals, particularly quartz and feldspar, to cumulatively store energy in the form of trapped charges produced by ionizing environmental radiation (Aitken, 1998).

Exposure of the mineral grains to sunlight causes the energy to be lost, a process also referred to as bleaching. Hence, the accumulation of the energy only begins once the sediment grains are buried. Collecting the mineral grains from the field and stimulating them in a laboratory allows the accumulated energy (paleodose) to be assessed. Typically for sediments, stimulation is performed using a light source to yield optically stimulated luminescence (OSL). Determining the rate at which the energy accumulated (dose rate) allows the burial age of the sediment to be calculated by dividing the paleodose by the dose rate. In natural environments, the burial of sediments is normally driven by geomorphic processes. Thus, luminescence dating ascertains time that has passed following the occurrence of a particular geomorphic episode. Accordingly, sediments that can be dated using luminescence methods essentially comprise clastic deposits that were appropriately bleached by sunlight before burial.

Full-fledged luminescence dating using standard protocols that employ laboratory-based luminescence readers is a time- and resource-intensive procedure. The method requires meticulous extraction of pure mineral separates (usually quartz or potassium feldspar) when using the coarse-grain method, or the fine-grain quartz approach. When dating silt-sized particles using feldspar signals, polymineralic grains within a specific grain size range are extracted instead. Furthermore, unique growth curves that reflect the relationship between the luminescence signal and the energy dose have to be constructed for each sample following the administration of artificial irradiation in order to calibrate the natural dose received by a sample. Apart from the requirement that the sample should have been adequately zeroed prior to being buried, sediment samples

have to fulfill a number of other pre-requisites before they can yield a reliable age. These include that electron traps which store the charge within the dosimeter lattices should not be exhausted or saturated prior to the end of the period being dated (e.g. Aitken, 1998), that initial zeroing has been complete, and that the sample has not been subject to post-depositional disturbance.

Because of the time- and resource-intensive character of conventional luminescence dating using standard instrumentation, many luminescence dating studies typically feature a relatively smaller number of ages than would be desirable under ideal circumstances. When working with complex geomorphological settings (e.g. Kocureck and Ewing, 2005), the limited spatial density of the ages is often insufficient to render a comprehensive understanding of the stratigraphic evolution of the landscape in question (e.g. Telfer, 2011; Munyikwa et al., 2012). The effect is exacerbated when collecting samples from depositional sequences that have no previous age information as the absence of an overarching chronological framework does not permit samples to be extracted from the most appropriate deposition units. Overall, these aspects highlight the necessity for acquiring appropriate chronological insight into the stratigraphic setting of any site under investigation as well as the potential benefits of conducting rigorous screening of samples that are ultimately selected for dating using standard luminescence dating protocols. Such precautions help prevent the expenditure of resources and time on samples that are not suitable for dating. Methods that have recently been used to provide such insight include the use of ground penetrating radar to examine internal dune structure (e.g. Bristow, et al., 2007).

Over the last decade, the development of functional portable OSL readers (e.g. Sanderson and Murphy, 2010; Kook et al. 2011) has provided researchers with a practical option to obtain luminescence signals from dosimeters relatively rapidly, compared to when using standard lab-based luminescence readers. The portable OSL reader, which can be acquired at a fraction of the cost of a standard OSL reader, enables researchers to attain a quick approximation of the luminescence energy stored in a sample for three main reasons. First, since the device is lightweight and portable, it can be easily transported to the field site: sample measurement can be conducted contemporaneously with sample collection. Second, the simplicity of the measurements, which in most cases can be performed without sample preheating, allows for quick results. Third and most importantly, the portable OSL reader can typically be used on bulk unprocessed sediment and this truncates the analytical process significantly compared to regular OSL dating. Overall, the combined effect of these aspects is that larger numbers of samples can be analyzed more rapidly and at much lower cost using the portable OSL reader. For any given study, the ability to analyze more samples introduces a greater spatial resolution of chronostratigraphic data which, in turn, affords practitioners prompt and improved contextual insight into geomorphic processes pertaining to landscape evolution.

Notably, however, there are a number of intrinsic drawbacks associated with the use of bulk, unseparated samples and portable luminescence readers compared to conversional lab-bound systems. These include:

- First, unlike the case with regular OSL readers, luminescence signals obtained with the portable instrument cannot readily be used to generate absolute ages using standard protocols. This is not least because signals from the unprocessed bulk samples often comprise mixed signals (e.g. mixed quartz and feldspar signals obtained under blue-OSL stimulation) because no mineralogical separations are performed prior to analysis. While pulsed methods have been used in some studies to partially separate quartz and feldspar signals (e.g. Kook et al., 2011) to date beyond approximations used in reconnaissance studies (e.g. Munyikwa and Brown, 2014; Stone et al., 2019) the combination of bulk screening and portable readers has not generally been used to produce full-fledged OSL ages. Bulk samples often contain a wide spectrum of grain sizes that may range from clay and silt fractions to coarse sand. In conventional OSL dating, specific grain size ranges are usually extracted and analyzed separately since they generally exhibit different luminescence characteristics, and their microdosimetry depends significantly on grain size and internal radioactivity levels. As outlined below, the lack of pre-heating capability or of irradiation sources in some portable systems while increasing portability precludes the field implementation of full-fledged OSL dating procedures.

- Second, when comparing raw portable OSL reader luminescence signals obtained from different units within a depositional sequence, direct comparison of signal intensities as indicators of relative chronology can only be made if the co-factor variables that influence signal intensity (e.g. mineralogy, dose rate, grain size,

aliquot size, degree of bleaching before burial, luminescence sensitivity, etc.) are constant between units. This is not always the case and therefore interpretation of co-factors and their potential variations is an important part of both initial field interpretation, and of subsequent stages of evaluation.

- Third, apart from applications that aim to approximate equivalent dose in samples, signals obtained using the portable OSL reader are often not routinely normalized for the range of variables that influence the signal intensity. This makes it difficult to compare raw signals from disparate sites, with most comparisons being confined to samples collected from proximal locations where dose rate, mineralogy, granulometry, etc. are thought to be consistent.

Nonetheless, despite these drawbacks, if the use of portable luminescence readers is considered complementary to the application of conventional OSL readers rather than a replacement, some of the potential disadvantages of the portable systems become inconsequential.

To highlight the utility of the portable OSL reader in geomorphological applications and to examine the current state of the science, this paper reviews studies that have been conducted over the last decade, identifying areas the investigations have focused on. In order to familiarize the reader with the basic layout of the portable OSL readers, design aspects of instruments developed over the last decade and their operational features are discussed. Studies in which the portable OSL reader has been used are then explored and these can generally be grouped into three main categories. The first comprises

studies in which portable OSL readers have been used to construct vertical luminescence profiles that show the variation of luminescence signals intensities with depth in depositional sequences. In settings where the main determinant of signal intensity is sediment age, the luminescence profiles serve as proxies for the chronostratigraphy (e.g. Sanderson and Murphy, 2010; Muñoz-Salinas et al., 2011; Kinnaird, et al., 2015). Hence, they can provide relative ages of depositional units and would be indispensable when formulating a sampling strategy for full-fledged dating. Additionally, portable OSL reader luminescence signals could provide insight into the geomorphic processes involved. In the second category, luminescence measurements obtained using a portable OSL reader are used to interpret sediment processes by examining bleaching characteristics of sediments from various depositional environments. The data are used to interpret sediment depositional pathways in order to gain a better understanding of landscape evolution. Sediment properties such as luminescence sensitivity can also be examined allowing them to be used as tracers for provenance studies (e.g. Gray et al., 2019; Lichtenberger et al., 2019). In the third category, luminescence signals from the portable OSL reader are calibrated in order to use them to approximate numerical burial ages of depositional units (e.g. Munyikwa and Brown, 2014; Stone et al., 2015; Stone et al., 2019). For each of the three categories, the environmental context in which the portable OSL reader was used is examined and the methodological aspects explored. The paper concludes with a brief look at future possible developments in methodological approaches as well as instrumental design. Overall, the scope of the paper and the case studies discussed are limited to geoscience applications completed so far. Thus, we do not examine theoretical and developmental aspects that would be more appropriate in a

separate dedicated review. This is tacit recognition that significant other research is in progress, most of which does not yet appear in the literature.

2. BASIC LAYOUT OF THE PORTABLE LUMINESCENCE READER

The potential benefits of being able to conduct a quick assessment of the luminescence properties of depositional sequences in the field has long been appreciated in geology and geomorphology. Concepts of portable luminescence readers that reached the development stage over the last three decades include instruments reported by Poolton et al. (1994), Takeuchi et al. (2008), Sanderson and Murphy (2010), and Kook et al. (2011). Each of these instruments is discussed briefly below. A portable OSL reader developed by Smetana et al. (2008) is largely intended for assessing exposure to UV radiation in work settings. Though the instrument could theoretically be adapted for assessing ionising radiation for geological applications, it will not be examined in this paper. In Table 1, potential advantages and drawbacks of each design are explored.

2.1 Portable OSL reader developed by Poolton et al. (1994)

The instrument developed by Poolton et al. (1994) weighed about 5 kg and was mainly designed for analyzing feldspar. However, with extensions, quartz could be examined too. The instrument featured a 30 mm photomultiplier (PM) tube (EMI bialkali photocathode, type 9924B) for photon detection after passing through a Schott BD39 filter. Sample

stimulation was provided by IR light emitting diodes (LEDs) supplying about 30 mM/cm^2 of power (880 nm) that targeted feldspar in continuous wave (CW) mode. Samples were held in a cartridge that could hold up to 12 samples in the form of pellets or sand grains. Bleaching capability was rendered by a blue Osram (DS/E 9-71) fluorescence lamp (400-550 nm) while Hg discharge UV lamps emitting around 50 μW/cm^2 at 254 nm (Osram HN10/UOFR or HNS10/UOZ) were used as an excitation source for signal normalisation. The instrument operated on a 12 V power source that could be supplied by the mains grid or by a portable source such as an automotive battery. A laptop computer provided a user interface. By adding a tungsten-halogen stimulation source to the system, the instrument could be expanded to also measure quartz OSL.

2.2 Portable OSL reader developed by Takeuchi et al. (2008)

Similar to the design by Poolton et al. (1994), the reader developed by Takeuchi et al. (2008) has a multiple sample holder with 13 positions. Weighing about 15 kg, the unit can perform both thermal (red thermoluminescence- RTL) and optical (OSL) stimulation. The optical stimulation is achieved by 16 blue (470 nm) LEDs, targeting quartz as well as 16 IR (890 nm) LEDs intended for feldspars. When conducting stimulation with the blue LEDs, SC42 (FUJI Photo Film) filters are used to screen the source signal before it reaches the sample. Four ceramic heaters enclosed in a brass casing provide the heating and can attain up to 600° C with electrical power under 128 W. A meta-packaged PM tube (Hamamatsu Photonics H7421-40) performs photon detection and OSL signals need

pass through a DUG11 filter (Schott) with a detection range of 300-400 nm before measurement. Artificial irradiation of samples is rendered using a miniature X-Ray generator (Oxford Eclipse-II-Reflection) that requires electrical power of around 3 W. The device can perform both CW and pulsed OSL measurements. Total power required to run the instrument without heating is about 50 W and when the laptop and heating are included, about 128 W is needed. In pulsed mode, pulse widths can range from 2-10 μs while the interval between the pulses ranges between 200-1600 μs. Pulsed-OSL signals are recorded between pulses.

2.3 The SUERC portable OSL reader (Sanderson and Murphy, 2010)

The portable OSL reader system used in all the studies discussed in this paper is the instrument developed by the Scottish Universities Environmental Research Centre (SUERC) and was described by Sanderson and Murphy (2010). We have not been able to identify any published studies that have employed the other three portable OSL readers and none of them appear to have progressed beyond the prototype instrument. We suspect the reason users have predominantly preferred the SUERC portable OSL reader so far is because of its ruggedness and operational simplicity. The basic layout of first- and second-generation designs of the SUERC portable OSL reader (up to ca. 2015) comprised three components: a detector-head mounted on a sample drawer, a control box with the operating switchgear, and a laptop computer to provide a user interface and a data logging system. The drawer holds samples that are introduced in 5-centimeter

diameter petri dishes or planchettes and the luminescence signal is obtained following stimulation using the appropriate source. The stimulating sources are housed just below the detector-head and normally comprise IR LEDs centred around 880 nm, as well as blue LEDs centred around 470 nm. Ports for the IR diodes are equipped with RG780 long pass filters while the blue LED ports are fitted with GG420 long pass filters. Following stimulation, the luminescence signal passes through UG11 filters and is detected by an ETL photon detector module. Fixed filters are used in the systems for ruggedness. But stimulation cones with different wavelength sources and detections bands have also been produced, allowing for different configurations. Sample stimulation can be in CW or pulsed mode. Pulse-on and pulse-off period can be set between 1 and 99 μs (Sanderson and Murphy, 2010). In addition to the switchgear, the control box also holds 4 NiMH 1.25 V batteries that can be used to provide power to the system when not connected to the mains grid. Overall, the instrument weighs under 5 kg. The third-generation SUERC portable OSL reader, which has been in operation since 2015, combines the detector head and sample tray as a single module (Figure 1). Other components including the electronics and operating software remain relatively similar to the second-generation design.

[Insert Figure 1]

2.4 Portable OSL reader developed by Kook et al. (2011)

The fourth and final luminescence reader examined in this paper is the portable instrument designed through collaboration between the Nordic Laboratory for Luminescence Dating and the Korea Basic Science Institute (KBSI). The device weighs about 8 kg and runs on a DC source (9-45V) or, alternatively, on grid power (AC). What differentiates this instrument from other portable OSL readers is a specially designed sampler that can be inserted into a depositional unit in its natural setting. This avoids the need for light-free conditions to enable the transfer of samples into a holder during measurement. The sampler can hold three samples and heat materials at 3°C s^{-1} up to 250°C using a heating coil (ThermoCoax) paired with a thermo sensor (RTD, Pt100). Other components of the system comprise the main body of the instrument which serves as the measurement table. Above the measurement table is a measurement head that houses the PM tube, LEDs for stimulation, as well as the X-ray source for artificial irradiation. For stimulating samples, the instrument only uses a blue OSL source comprising 24 W LEDs centred around 470 nm for analyzing quartz. A long pass GG420 Schott filter is placed in front of the LEDs. Luminescence signals are detected by a 30 mm bialkali PM tube (9125B, ET Enterprises Limited) after passing through a U340 filter (Hoya). As with the SUERC reader, Kook et al.'s (2011) instrument can also operate in both CW and pulsed mode. When in pulsed mode, pulse-on and pulse-off period can be set anywhere between 1 and 65,535 μs. Sample heating capability allows TL analysis to be made. Apart from measuring regular luminescence, the device can also measure radioluminescence, which is the signal obtained while a sample is irradiated by an ionizing source.

[Insert Table 1]

2.5 Portable OSL reader measurement modes

Both regular and portable OSL readers are capable of performing measurements on processed as well as on unprocessed samples. Bulk samples are usually analyzed when prompt data are required for reconnaissance or screening purposes. Portable OSL readers optimize the ability to acquire speedy results from bulk samples because they can be taken into the field where near real-time data can be incorporated into the sampling strategy. Sample mounting is also far simpler in some portable OSL readers than in the standard lab-bound varieties. In many depositional settings, bulk materials would include both quartz and feldspar. Hence, the measurement strategy that is usually adopted aims to target grains of quartz or feldspar in separate measurement steps performed at room temperature. Since IR stimulation has a negligible effect on the fast component of quartz below 125°C (Spooner and Questiaux, 1989; Short and Huntley, 1992; Bailey, 1998; Thomsen et al., 2008), measurement on polymineralic aliquots is typically conducted by first stimulating using an IR source after which blue OSL stimulation may follow. Notably, blue light causes luminescence in both feldspars and quartz. However, a significant proportion of blue-sensitive traps in feldspar are also depleted by prolonged exposure to IR stimulation (Duller and Bøtter Jensen, 1993; Clark and Sanderson, 1994; Galloway,

1994; Jain and Singhvi, 2001). Hence, stimulating the sample with blue-OSL after IR stimulation may enhance the quartz contribution from bulk samples. The OSL signal obtained from this sequence of analysis is referred to as a post-IR blue OSL signal (e.g. Roberts and Wintle, 2001; Wallinga et al., 2002). When using the SUERC reader in CW mode, it is possible to use the sequence editor in the user software to vary both the dark count and the times of exposure to IR or OSL sources. The dark count measurement mode provides the machine background count rate in the absence of stimulation, and defines the statistical detection limits of detection of weak luminescence signals. Dark counts originating from the photomultiplier comprise both thermal and non-thermal components (Carter et al, 2018). The measurement sequence can also be used to record low level [phosphorescence emitted from samples when first introduced to the system, or post-stimulation phosphorescence, which is emitted at low levels after the samples have been measured. Dark count measurements can be alternated with stimulation measurement modes. Stimulation times can vary from 0-999 s. Typical measurement sequences involve a 10 s dark count followed by 60-80 s IRSL or OSL stimulation after which another dark count is taken. Post-stimulation phosphorescence (PSP) can also be monitored if needed.

Quartz and feldspar signal separation under blue OSL stimulation can also be performed by pulsing the OSL signal. Luminescence of feldspars includes shorter lifetimes in the nanosecond to several microsecond timescales than those associated with the main quartz OSL emissions (e.g. Sanderson & Clark 1994, Denby et al., 2006; Thomsen et al., 2008; Ankjaergaard et al., 2015). Hence, the suggestion that in pulsed mode, by

347 performing the measurement of the sample signal only during the pulse-off period and
348 delaying the onset of the measurement (e.g. by 2-5 μs), the faster feldspar signal
349 components can be suppressed while allowing quartz dominant signals to be measured.
350 Kook et al. (2011) primarily used this approach to concentrate quartz signals from
351 samples that contain both quartz and feldspar grains.
352
353 Typical IRSL and post-IR blue OSL shine-down curves obtained using a SUERC reader
354 in both CW and pulsed modes are shown in Figure 2. The slow depletion of the signals
355 are the result of the relatively low power from the stimulation sources, coupled with the
356 deliberately large sample areas, and the use of thick samples (e.g. Stone et al., 2015).
357 Additionally, feldspar contribution to the post-IR blue OSL signal could also be influencing
358 the depletion rate (e.g. Duller, 2003). As detailed above, when in pulsed mode, the
359 SUERC portable OSL reader cannot gate the signal measurement to pulse-off periods
360 only such that feldspar emissions, if present, are not excluded. Pulsed stimulation using
361 a SUERC portable OSL reader was reported by Muñoz-Salinas et al. (2011). In this case
362 pulse-on window was synchronized with measurements on a 15 microsecond gate, thus
363 autosubtracting dark count signals and any long-term luminescence recombination.
364
365
366 [Insert Figure 2]
367
368

IRSL or OSL measurements from the portable OSL reader are often presented as integrated signal intensities over the period of measurement. It is also possible to calculate signal depletion ratios, IRSL/OSL ratios, post-stimulation IRSL and OSL PSP (Sanderson and Murphy, 2010; Kinnaird et al., 2015; Kinnaird et al., 2017). The signal depletion index is calculated as the ratio of the luminescence intensity in the first half of the stimulation period divided by the intensity in the second half. Factors that can influence the depletion rate of bulk samples include the mineralogy of the sample, grain size distribution, color of the grains (or coatings) as well as the extent to which a sample contains mixtures of grains that were well beached and those that were partially bleached prior to the last burial event (Sanderson and Murphy, 2010). Depletion ratios of sediments that were well bleached prior to burial would be higher than for sediments that were not completely bleached since inherited signals deplete less rapidly. Overall, the use of depletion ratios allows a determination to be made if variations in signal intensity down a sequence are influenced by factors other than burial age or dose rate. For instance, Sanderson et al. (2010) examined depletion ratios for a stratigraphic sequence comprising Neolithic ditch fills at Cava Petrilli, Italy. Results showed the ratios were relatively constant down the section, suggesting that bulk properties such as sediment color and grain size did not lead to significant variations in luminescence sensitivity between the different depositional units. In another study, examining agricultural terraces from Catalonia in eastern Spain, Kinnaird et al. (2017) noted that depletion ratios provided an indication that the units were better bleached at deposition, and used this to identify anthropogenic and natural fills. In essence, the depletion ratio allows main determinants of the variations in luminescence intensity to be identified.

Similarly, if IRSL measurements are targeted at feldspar, and OSL at quartz, comparisons of IRSL/OSL ratios between different samples could be seen as a reflection of variations in relative concentrations of feldspar to quartz within the samples. Stratigraphic sections that feature homogenous IRSL/OSL ratios (e.g. Munyikwa et al., 2012) would suggest that proportions of feldspar relative to quartz are constant down the sequence, and that variations in luminescence intensity arise from other influences such as burial age or dose rate. Conversely, sections where IRSL/OSL values fluctuate point to variations in the relative concentrations of feldspar to quartz. Such variations have been attributed to differences in the degree of weathering (e.g. Sanderson and Murphy, 2010) since feldspars disintegrate more readily than quartz when exposed to the elements.

3. CONTEXTUALIZING SEDIMENT STRATIGRAPHY BY LUMINESCENCE PROFILING USING THE PORTABLE OSL READER

3.1 Luminescence profiling using conventional OSL readers

Before discussing luminescence profiling using portable OSL readers, it is pertinent to examine profiling that can be performed using standard lab-bound OSL readers. When initially proposed, the primary aim of profiling using standard OSL readers was to acquire preliminary insight into depositional contexts of stratigraphic sites and to assess the suitability of samples for conventional OSL dating (e.g. Sanderson et al., 2001; 2003;

Burbidge et al., 2007). A key aspect of this approach is the use of bulk or partially processed samples as well as abbreviated procedures for determining D_e in order to expedite the evaluation. For instance, working on Paleolithic archeological sites in Russia, Burbidge et al. (2007) encountered a range of stratigraphic sequences some of which did not appear to be suitable for dating using OSL. Hence, an initial evaluation of the sites was performed to identify samples worth dating using full-fledged OSL protocols. Aspects the preliminary assessment aimed to address included the extent to which sediment signals had been reset prior to the last burial episode and the identification of discrete depositional phases contained in the sections. Ages that had been obtained from the sequences in previous studies using $^{40}Ar/^{39}Ar$ dating, ^{14}C, $\delta^{18}O$ stratigraphy, magnetostratigraphy, as well as conventional OSL provided independent age controls for the sections. As part of the profiling, samples collected from the stratigraphic sites were divided into three separate subpopulations: polymineral silt (4-12 μm), polymineral sand (90-250 μm), as well as quartz-enriched sand (90-250 μm). In this way, the influence of grain size and mineralogy on luminescence signals was examined. Each of the three subpopulations was measured using IRSL, post-IR OSL and TL on a conventional OSL reader, and equivalent doses (D_e) calculated. The D_e determinations employed an abbreviated regenerative dose method that only used two aliquots. Values that were obtained were then plotted to show the variation of D_e with depth for each section. Results indicated that data obtained using coarse-gained polymineral sand were relatively consistent with those obtained using quartz-enriched sand, suggesting that rapid measurements using partially processed samples and abbreviated protocols could produce valuable preliminary information. Furthermore, the approach showed that

438 combining rapidly acquired profiling results from a given site with a few ages obtained
439 using standard OSL protocols could yield a detailed chronostratigraphic framework,
440 ultimately conserving time, effort and resources.
441
442 Other studies that have examined ways of conducting preliminary studies using standard
443 OSL readers include work by Hamel and Huntley (2003), who used IRSL to estimate
444 equivalent dose in unprocessed sand and noted that measurements made on the
445 samples returned D_e estimates that were reliable approximations of values obtained using
446 standard OSL protocols. Possible reasons for variations of results between the two
447 approaches that were cited included the broader grain size range in the raw samples and
448 the possible presence of other minerals that responded to IRSL, unlike in the processed
449 samples where only K-feldspar was present.
450
451 Beyond investigating depositional sites using luminescence profiling for the presence of
452 samples suitable for dating (e.g. Sanderson et al., 2001, 2003; Burbidge, 2007), signals
453 obtained from quartz in bulk samples using standard OSL readers have also been used
454 to determine OSL range-finder ages that give preliminary age estimates (e.g. Roberts et
455 al., 2009; Durcan et al., 2010). Sand from a dune from Namib desert as well as from a
456 coastal dune from the UK were analyzed by Roberts et al. (2009), by comparing D_e values
457 obtained from raw samples to values yielded by pure quartz from the same sample.
458 Results showed that raw samples returned D_e values within 65 -70% of the D_e obtained
459 from pure quartz. When the bulk sample was first exposed to IR stimulation for 500 s
460 before post-IR blue OSL stimulation, the D_e values calculated were within 82-90% of the

value obtained from pure quartz separates. Hence, this suggested that reliable range-finder ages could be estimated on quartz in raw samples, especially using post-IR OSL stimulation. However, the same result was not replicated in another study. Working with samples from eastern Pakistan, Durcan et al. (2010) noted that the initial IR stimulation could not adequately deplete the feldspar signal such that post-IR blue OSL signals continued to be dominated by feldspar emissions. As a result, further chemical treatment of the sample was required to eliminate feldspar before measurement. In other studies, pulsed OSL signals using standard OSL readers (e.g. Thomsen et al., 2008) have been used to measure quartz signals in samples with polymineral grains in combination with minimal sample processing. Results showed close agreement between samples prepared using conventional protocols and those that had simply been washed and sieved.

Overall, what all these methods highlight is the inherent value of preliminary screening methods that can be used to identify samples that are worth expending resources and time on. They also show that useful information about the dose stored in a sample can be ascertained by performing measurements on bulk samples with minimal or no preprocessing. Ultimately, the efforts allow the extraction of maximum benefits from a given study.

3.2 Luminescence profiling using portable OSL readers

484 The portable OSL reader can be used to collect data for luminescence profiling as with
485 the conventional OSL reader. The main advantage of the portable OSL reader in this
486 case, as highlighted earlier, is that it can be taken to the field, allowing for rapid decisions
487 to be made, especially if the information is to be factored into a larger sampling program
488 for conventional OSL dating. However, the lack of an internal irradiation source in some
489 portable readers means that such devices cannot be used to normalize luminescence
490 signals for grain size variation or sample size using a test dose administered internally by
491 the reader. Despite that constraint, as will be shown in case studies examined below,
492 profiling using the portable OSL reader can provide invaluable preliminary insight into
493 cryptostratigraphic features of late Quaternary depositional systems (Sanderson and
494 Murphy, 2010). In most cases performed to date, profiles derived using portable reader
495 data are obtained by constructing vertical sections that show the variation of
496 luminescence signal intensities with depth or, in essence, luminescence stratigraphies
497 (e.g. Sanderson and Murphy, 2010). The signals plotted in a luminescence profile could
498 be either IRSL, or OSL net signal intensities that are recorded during measurement.
499 Depletion ratios and IRSL/OSL ratios can also be presented in profile form. As detailed
500 above, luminescence intensities recorded from the bulk samples depend on variables that
501 include a) the local dose rate, b) inherited dose at time of burial, c) luminescence
502 sensitivity of the mineral grains, d) time that has lapsed since burial age of the sediment,
503 and e) mineral composition. In a depositional sequence where all these variables are
504 constant, apart from the duration of burial, the profile would essentially be representative
505 of the chronostratigraphy. Thus, unless the sequence has experienced post-depositional
506 disturbance, the luminescence profile should exhibit increasing signal intensities with

507 depth, commensurate with increasing age as implied by the stratigraphic principle of
508 superposition. Figure 3a is an example of a relatively homogenous sequence in terms of
509 grain size, mineralogy and, to a large extent, dose rate that was deposited over time in a
510 postglacial aeolian dune in Alberta, Canada (Munyikwa et al., 2012). Both the IRSL and
511 post-IR blue OSL signals (CW mode) increase gradually with depth. However, the
512 IRSL/post-IR blue OSL ratio is relatively uniform down the profile, suggesting minimal
513 variation in mineralogy. This indicates that burial age is the most important determinant
514 of signal intensity. In the example depicted in Figure 3a, the aeolian dune sediment was
515 well bleached prior to burial as it shows gradual growth in signal intensity from the top
516 downwards; with the slope on the signal-depth progression providing some insight on the
517 sedimentation rate. Figure 3b reported by Portenga et al. (2016) shows a similar trend. In
518 this instance, fine-grained sediments deposited by fluvial processes in a swampy meadow
519 wetland environment in southeastern Australia show IRSL and post-IR blue OSL signals
520 (CW mode) that increase gradually with depth. The shallow and low-energy environment
521 is thought to have allowed complete bleaching of the sediment prior to burial (Portenga
522 et al., 2016). Hence, since the sediment is assumed to have a common provenance
523 upstream, burial age is also thought to be the dominant influence on signal intensity.
524 Comparable results were reported in similar fluvial deposits from the same region by
525 Muñoz-Salinas et al. (2014). In some settings, sediments are deposited relatively quickly
526 so that the age difference between sediment at the base and at the top of the sequence
527 is minimal. In such cases, the luminescence profiles exhibit signal intensities that are
528 relatively constant throughout the depositional column as in Figure 4 recorded (CW mode)
529 for a coastal dune at Holkham in Norfolk County, UK (Bateman et al., 2015).

[Insert Figure 3]

[Insert Figure 4]

There are cases where poorly bleached or increasingly older sediment can be emplaced above younger deposits. Such profiles would exhibit signals that increase in intensity up the profile, which would be an inverted form of Figure 3. Studies that have reported such inverted profiles include work by Sanderson and Murphy (2010) where multi-wave tsunami events in Thailand eroded increasingly older sediment and deposited it onshore without any significant signal zeroing. Similarly, inverted signal distribution was noted by Sanderson and Murphy (2010) in Italy where what are thought to be excavation tailings were used as backfill overlying a lower archaeological fill after the abandonment of a Neolithic enclosure ditch (Figure 5a). Sanderson and Murphy (2010) suggest that the higher signal intensities (CW mode) in the upper fill indicate that the back filling may have been rapid such that limited signal zeroing occurred. Thus, the upper fill likely contains sediment of mixed age. Luminescence dating using standard protocols of samples from the upper fill and lower fill returned ages that suggest a slightly older age for the upper fill, consistent with the trend from the portable reader signals (Figure 5a). Higher

553 IRSL/post-IR OSL ratios in the upper fill are also thought to indicate a higher feldspar
554 content because the degree of weathering is not as intense as in the lower fill. Hence,
555 overall, higher portable reader signals in this case were influenced by a combination of
556 factors including degree of signal resetting (and time since last exposure) and feldspar
557 content. Depletion ratios were reported to be uniform throughout the sequence,
558 suggesting that color or grain size did not have major influence on the signal intensities.
559 In south-eastern Australia, Muñoz-Salinas et al. (2014) and Portenga et al. (2016)
560 reported a more or less similar trend where a finer grained swampy meadow (SM) deposit
561 was overlain by a coarser post (European) settlement alluvium (PSA). Portable
562 luminescence signals obtained (CW mode) showed that signal intensities in the SM unit
563 started at very low levels in the upper part and increased steadily down the unit (Figure
564 5b). In the overlying PSA unit, however, the signals were several orders of magnitude
565 higher and displayed much scatter. Measurement with a field dosimeter showed that there
566 were no significant differences in dose rates between the SM and PSA units. Hence,
567 Muñoz-Salinas et al. (2014) concluded that higher signals in the PSA unit likely resulted
568 from poor bleaching of the sediment at the time of deposition and also because there
569 were differences in mineralogy between the SM and PSA units. Poor bleaching was
570 thought to be related to grain size as well as to transport mechanisms. Coarser grains
571 that are transported under turbid conditions are less likely to be reset by daylight
572 compared to finer grains that were deposited by slow moving dilute flow. Overall, Munoz-
573 Salinas et al. (2014) concluded that, unlike the PSA alluvium, SM deposits were
574 appropriate for dating using regular OSL protocols. Samples retrieved from depths of 103

575 cm and 163 cm returned ages of ca. 2.4 and 5.2 ka respectively, consistent with the higher
576 portable reader signals with increasing depth.
577
578
579 [Insert Figure 5]
580
581
582 Luminescence profiling can also effectively delineate depositional units of different age
583 within a given depositional sequence. As in all profiling studies, the analysis would ideally
584 require signals to be normalized for the effects of variables such as dose rate or sample
585 size prior to comparing the signals for age variation down the profile. For instance, sample
586 aliquots could be weighed accurately prior to conducting luminescence measurements
587 and dose rates could be determined at sampling positions using a portable gamma ray
588 spectrometer. Normalizing the signals for dose rate and sample size would then enable
589 a profile with a time-dominant signature to be obtained, unless other variables such as
590 mineralogical changes or inadequate bleaching are also involved. In a profile that features
591 signals with time-dominant variations, units of different age would be distinguishable as
592 segments of the profile separated by sudden increases in signal intensities. Accordingly,
593 where unconformities or extended gaps in depositional chronology occur, luminescence
594 profiles should display abrupt changes in signal intensities across the uniformities.
595 Multiple profiling studies have been performed with the primary aim of identifying distinct
596 stratigraphic units in depositional sequences. For instance, Muñoz-Salinas et al. (2011),
597 identified a major unconformity in fluvial sediments from an abandoned channel in the

598 Mekong Delta in Cambodia using this approach (Figure 6a). Visual assessment had
599 identified four depositional units (I-IV) based on color. However, luminescence profiling
600 using the portable reader showed that units I and II in the upper part had relatively similar
601 signal intensities but were significantly different from units III and IV which were both
602 characterized by higher signals and had much higher scatter. A good linear correlation of
603 the signal intensities in units I and II was deemed to indicate that the units were well-
604 bleached at the time of deposition. The scatter in units III and IV was thought to be a
605 product of bioturbation, given the pervasive presence of worm burrows. Though grain size
606 in unit I was notably coarser than in unit II, the grain size in units III and IV was relatively
607 similar to that in unit II. Hence, grain size did not appear to be the main reason for the
608 difference in signal intensities between units I/II and III/IV. Magnetic susceptibility
609 measurements showed that units III and IV had significantly different susceptibility
610 compared to units I/II, pointing to a difference in mineralogy and provenance.
611 Furthermore, radiocarbon dating of invertebrate shells from units I and II returned modern
612 ages, which accords with the very low signal intensities. From unit III, however, organic
613 matter returned ages of 5.9 ka and 6.3 ka while from unit IV, an age of 5.7 ka was
614 obtained. Hence, the differences in signal intensities (CW mode) between I/II and III/IV
615 was largely deemed to result from differences in age, though mineralogy may have also
616 had some influence. In Mexico, an interface between two lahars from 1997 and 2001
617 generated by eruptions of the Popocatépetl volcano was also identified using a similar
618 method (Muñoz-Salinas et al., 2011). Because of the young ages of the lahars, portable
619 luminescence profiling of the deposits returned relatively low signals. However, signals
620 from the 2001 deposits were relatively uniform down the profile whereas the 1997 lahar

621 fluctuated significantly. Muñoz-Salinas et al. (2011) suggested that the differences in the
622 signals was a product of differences in the provenance of the two lahars. The 2001 lahar
623 contains homogenous sediment from a single source whereas the 1997 lahar comprises
624 heterogeneous material from multiple sources. As a result, the differences in
625 luminescence characteristics down each unit enabled the transition between the two units
626 to be delineated.
627
628 Luminescence profiling using a portable OSL reader also enabled Rother et al. (2019) to
629 identify a major unconformity between Eemian penultimate interglacial deposits and late
630 glacial cover sands in northeastern Germany (Figure 6b). Deposits at the site were
631 classified into 6 main units. Unit 1 at the base was fine sand (possibly glaciofluvial) that
632 overlay till. Above the basal sand unit was peat that constituted unit 2. Units 3 - 5 overlay
633 the peat and comprised fine-grained laminated lacustrine sediment thought to have been
634 deposited in a depression in dead ice. Overlying the lacustrine deposits, Unit 6 comprised
635 poorly sorted medium-grained sand containing some larger clasts as well as ventifacts.
636 Luminescence profiling (CW mode) showed two main segments. Signal intensities for unit
637 6 were fairly consistent throughout the unit. Across the boundary, into units 1-5, signal
638 intensities increase by 2 orders of magnitude, which pointed to a major unconformity
639 (Figure 6b). While mineralogy, grain size, and dose rate could be possible contributors to
640 the differences in signal intensity, depletion ratios for IRSL and blue OSL were relatively
641 uniform throughout the entire section, showing that sediment bulk properties were not a
642 factor. Also, importantly, OSL dating of 4 samples from unit 6 returned a weighted mean
643 age of 14.2 ± 0.5 ka while ^{320}Th/U dating of samples from the lacustrine sediment returned

644 a corrected age of 118 ± 7/6 ka and 114 ± 6/5 ka. Hence, in this instance, a major
645 influence for the differences in signal intensity was confirmed to be burial age. Rother et
646 al. (2019) concluded that the lacustrine deposits (units 2-5) were deposited during the
647 Eemian interglacial while unit 6 comprised periglacial cover sands deposited by aeolian
648 processes towards the end of the last glacial period.
649
650 Other studies that have employed luminescence profiling to identify discrete units in
651 depositional sequences include work by Munyikwa et al. (2012), Muñoz-Salinas et al.
652 (2013; 2014), Mills et al. (2014), Palamakumbura et al. (2016), Portenga and Bishop
653 (2016), Portenga et al. (2016), Kinnaird et al. (2017), Porat et al. (2019) and Rother et al.
654 (2019). In many cases the differences in the signals have been related to either the
655 depositional age or to the bleaching that occurred prior to burial. Bleaching characteristics
656 are also usually related to the sediment transport and depositional mechanisms.
657
658
659 [Insert Figure 6]
660
661
662 Table 2 outlines luminescence studies that have employed profiling as part of efforts to
663 contextualize the stratigraphy at respective depositional sites. As indicated earlier, in all
664 instances, the portable OSL reader used is the instrument developed by SUERC. For
665 discussion purposes the studies are grouped by environment of deposition, including
666 coastal, fluvial, aeolian, glaciolacustrine, and offshore marine settings. While the

667 environments may differ, the applications and techniques used in the studies are largely
668 similar. In most studies, the main purpose for employing profiling has been to provide
669 insight into the environment of deposition and to inform sample collection for
670 luminescence dating using standard protocols. Hence, the identification of units that
671 appear to have been well-zeroed before burial is the objective of many studies.
672
673 Some studies combine observations in the field with subsequent laboratory
674 characterization (cf. Burbidge et al., 2007) to 'calibrate' the field profiles, and extend the
675 sediment chronologies into the adjacent stratigraphies (e.g. Kinnard et al., 2017, 2019);
676 or, alternatively, by interpreting signal intensities in light of OSL ages (Porat et al., 2019).
677 Age approximation using portable OSL signals is discussed in greater detail later in this
678 paper.
679
680
681 [Insert Table 2]
682
683
684 From the range of studies outlined in Table 2, it is evident that there is a broad range of
685 settings in which the portable OSL can be applied. The only major requirements are that
686 the deposits being analyzed should contain a dosimeter (normally quartz or feldspar) that
687 was emplaced by geomorphic processes in both space and time. However, there are
688 some environments that are particularly amenable to profiling using the portable OSL
689 reader. Ideally, the sequences being investigated should have grain sizes, mineralogy,

690 luminescence sensitivity and dose rates that are relatively consistent down the profile
691 such that only burial age is the major determinant of signal intensity. Sediments that were
692 zeroed effectively prior to burial are also preferable as it provides a temporal datum above
693 which stored dose can accumulate following deposition. As with conventional OSL dating,
694 aeolian deposits are particularly suitable for profiling because aeolian deposits are often
695 well-bleached at deposition and wind transport sorts grains into narrow size ranges such
696 as dune sand, or silt-sized loess. Fluvial deposits, on the other hand, are not always well-
697 bleached and sediment grain size ranges can be more variable (e.g. Rittenour, 2008;
698 Cunningham and Wallinga, 2012). With glacial deposits, bleaching is even more limited
699 (e.g. King et al., 2014), though outwash sands would offer the best opportunity for profiling
700 in such environments.
701
702
703 **4. INTERPRETING DEPOSITIONAL HISTORIES USING LUMINESCENCE SIGNALS**
704
705 As highlighted above, complete zeroing of dose stored in sediment is not always possible
706 before burial. Different sediment transport mechanisms are often associated with
707 bleaching opportunities that are dissimilar. For effective bleaching to occur, sediment
708 should be exposed to adequate sunlight (or heating, in the case of baked sediments).
709 High intensity processes such as turbidity currents or debris flows do not allow adequate
710 time for zeroing (e.g. Muñoz-Salinas et al., 2017a, 2017b, 2018) whereas gradual
711 processes at the earth's surface, such as subaerial transport of sediments through
712 saltation that occurs with aeolian dune sediments (e.g. Singhvi and Porat, 2008), offer the

best opportunities. In this section, studies that have explored bleaching characteristics of different environments using portable OSL readers are examined. The studies are grouped into two main categories. The first looks at studies where the extent of signal resetting associated with some depositional environments were investigated (e.g. King et al., 2014; Muñoz-Salinas et al., 2018). The second looks at studies where bleaching characteristics were used to elucidate geomorphic processes (Stang et al., 2012; Castillo et al., 2014; Muñoz-Salinas, 2017b, 2018). The use of luminescence signals as sediment tracers is also examined briefly.

4.1 Examining bleaching characteristics of depositional environments

The analysis of inherited luminescence signal characteristics of modern sedimentary environments using a portable OSL reader enables the identification of optimal bleaching conditions for a given depositional system. Insight into bleaching characteristics acquired from such investigations facilitates informed targeting when sampling for conventional OSL dating is directed at fossil landforms. For instance, Muñoz-Salinas et al. (2017a) investigated bleaching in sediments younger than 2 ka from fluvial, coastal, and volcanic environments from Mexico using a portable OSL reader. Samples were analyzed using IRSL and blue OSL stimulation in CW mode. As expected, the results generally showed that sediments transported by debris flows had the highest residual signals since the opportunity for bleaching was limited. It was also noted that IRSL signals from volcanic ash and coastal deposits (beach and dune sand) were characterized by low scatter. The

736 blue OSL signal, however, had significant scatter for both coastal and volcanic sediments.
737 For coastal deposits, Munoz-Salinas et al. (2017a) attributed the scatter to charge transfer
738 whereas for volcanic deposits, low quartz sensitivity was suspected. The fluvial deposit
739 exhibited a high degree of scatter with both IRSL and blue OSL stimulation, possibly from
740 sediment mixing.
741
742 A more focused study that examined bleaching mechanisms was conducted by King et
743 al. (2014) who investigated catchment-scale variability in residual signals of modern
744 glacial sediments in Jostedalen, southern Norway. Samples were collected from shallow
745 depths in glaciofluvial bars including braided bars and side-attached bars from four
746 different catchments. Additional samples were also collected from subglacial, paraglacial,
747 and avalanche deposits that served as sources for the glaciofluvial sediments. Sample
748 measurement was performed using a portable OSL reader (CW mode) and, overall,
749 residual signals in bar environments fell as the glaciofluvial sediment was carried further
750 from the ice margin or from the sediment source (e.g. Figure 7). Slope failure deposits
751 and sheet wash deposits had some of the highest residuals since such rapid depositional
752 processes offered limited opportunity for exposure to sunlight (King et al., 2014). For
753 glaciofluvial deposits, residual signal intensities also depended on morphological aspects
754 of the depositional feature. For instance, braid-bar-head deposits generally had the
755 highest residual signal intensities while braid-bar-mid, braid-bar-tails and side-attached
756 bars had some of the lowest. For some sites, settings where poorly bleached sediment
757 was continuously added to the sediment load as it moved downstream resulted in a high
758 degree of luminescence signal variability. Thus, the results confirmed that high magnitude

events of low frequency such as turbulent flows had poor sediment bleaching opportunities whereas low magnitude events that occurred with a higher frequency, such as deposition in braid-bars-mid and tails, offered greater chances for bleaching (King et al., 2014).

Overall, the studies by King et al. (2014) and Munoz-Salinas et al. (2017a) demonstrated the utility of the portable luminescence reader to rapidly characterise bleaching of sediment in a range of modern depositional settings. Observations from such studies can inform sampling strategies in conventional OSL dating of fossil landforms.

[Insert Figure 7]

4.2 Elucidating depositional processes using portable reader luminescence signals

Beyond screening samples for conventional OSL dating, luminescence signal characteristics acquired using a portable OSL reader have also been used to infer geomorphic processes associated with depositional sequences. In a study by Stang et al. (2012), the instrument was used to assess soil mixing processes and rates at a site in the San Gabriel Mountains, California. The study had noted that in order to understand processes that influence rates of weathering and erosion at some scales, there was a need to evaluate the relative significance of mechanisms by which clastic particles are

translocated within soil profiles and their rates. Samples were collected at constant intervals from three soil profiles on hillslopes within a 100 m radius. Using the portable OSL reader, IRSL and post-IR blue OSL signals were obtained from each sample in CW mode. To allow a measurement of relative time, an IRSL growth curve was constructed using a conventional OSL reader and select bulk samples from the study area. The growth curve was used to convert dose values into 'effective age' estimates. Figure 8 outlines plots of effective age versus depth for the three monoliths sampled in the study. Low 'effective ages' were interpreted as denoting episodes during which sediment was close to the surface such that the grains were bleached by sunlight or heated by wildfires before being subsequently translocated downward.

[Insert Figure 8]

In another study that aimed to unravel sediment transport mechanisms, Castillo et al. (2014) used signal intensities acquired using a portable OSL reader to compare rates of erosion that followed late Cenozoic differential tectonic uplift of the Jalisco Block in western Mexico. The results showed that high IRSL signal intensities were recorded for samples from the northern sector of the Jalisco Block while lower intensities were noticed in the southwest. Though dose rates were not provided, Castillo et al. (2014) argued that the high signal intensities from the northern sector resulted from higher rates of uplift that contributed a higher sediment load while lowering opportunities for bleaching. Lower rates

of uplift in the southern sector, on the other hand, produced lower sediment loads and gentler flows which were associated with greater chances of bleaching. Similar results were reported by Munoz-Salinas et al (2017a) who examined sediment in rivers that cross two major faults in the Sierra De Juárez mountains in southern Mexico. Here, results showed that inherited portable OSL signals were higher in basins with steeper slopes compared to those with more gentle relief. Hence, the signals from steeper slopes were consistent with sediment transported in debris flows or in hyper-concentrated flows where turbidity was significant.

Mechanisms of sediment transport in other fluvial settings were examined by Muñoz-Salinas et al. (2018) who compared rates of erosion between areas in central Mexico under conservation with those where natural vegetation was allowed to grow. In this study too, streams characterized by hyper-concentrated or debris flows did not exhibit much bleaching. Additionally, streams where fresh sediment that is poorly bleached was continuously incorporated into the stream exhibited luminescence intensities that increased downstream (Figure 9). Overall, the results showed that conservation efforts in the area were unsuccessful as they caused landscape instability compared to areas with natural vegetation (Munoz-Salinas et al., 2018). In the Wadi Suf in Jordan, Lichtenberger et al. (2019) analyzed three profiles along the Chrysorrhoas River and noted that luminescence signal intensities increased downstream. However, in this instance the higher signals were attributed to increase in luminescence sensitivity following repeated cycles of deposition, erosion and transportation (Lichtenberger et al., 2019).

Table 3 summarizes studies that have explored sediment bleaching using a portable OSL reader. The application of luminescence as a sediment tracer and provenance tool has been reviewed by Gray et al. (2019). Though the review does not focus exclusively on the use of portable readers, it highlights areas where luminescence could be used to identify source lithologies and transport mechanisms based on luminescence characteristics.

[Insert Figure 9]

[Insert Table 3]

5. APPROXIMATING SEDIMENT BURIAL AGE USING A PORTABLE OSL READER

An area that has seen some emerging applications in efforts to expand the utility of portable OSL readers has been the calibration of portable signals so that they can be used for approximating numerical ages, as opposed to simply providing relative chronology. A number of approaches have been used, ranging from the application of standardised growth curves (SGCs) generated using normalised portable OSL reader signals to approximate the equivalent dose (e.g. Munyikwa and Brown, 2014), to the

851 construction of calibration curves that use samples whose ages have been determined
852 using standard luminescence dating protocols and have also had their signals measured
853 using portable luminescence readers (e.g. Stone et al., 2015, 2019). While the methods
854 have been applied primarily to inland aeolian deposits (e.g. Munyikwa and Brown, 2014;
855 Stone et al., 2015; 2019), age estimation using portable OSL readers has also been
856 extended to coastal sediments (e.g. Brill et al., 2016), and to wetland deposits that
857 comprise aeolian and fluvial sediments (e.g. Gray et al., 2018). With wetland deposits,
858 the possibility of sediment mixing and partial bleaching that is associated with such
859 environments appears to introduce significant scatter in the data, likely more than would
860 be expected with well-bleached aeolian deposits. Nonetheless, as range finders that
861 assist targeting of sampling and further follow-up, the age approximations provide a useful
862 aid in luminescence studies. Each of these approaches is discussed below.
863
864 5.1 Approximating D_e by constructing SGCs using portable OSL reader signals
865
866 Modern versions of SGCs were proposed by Roberts and Duller (2004) as an approach
867 that could truncate age determination procedures in luminescence dating assessment,
868 especially when conducting reconnaissance studies. With SGCs, luminescence growth
869 curves are constructed using normalized signals and once a curve is constructed, the D_e
870 of a natural sample of unknown age is determined by simply acquiring a normalised
871 natural signal which is then compared with the SGC to derive a corresponding D_e. In
872 essence, the use of an SGC negates the construction of a unique growth curve for each
873 sample, which is the standard procedure in luminescence dating. Typically, SGCs are

874 appropriate for sediments that share similar luminescence properties. Hence, they are
875 regionally applicable at best.
876
877 The combination of an SGC with a portable OSL reader that can analyze bulk samples
878 appears to be an attractive concept as it abbreviates the process of age estimating
879 significantly (Munyikwa and Brown, 2014). There are two main challenges that are
880 associated with constructing SGCs using portable OSL reader signals. The first is that a
881 source of artificial radiation is required for constructing the growth curve as well for
882 administering test doses for signal normalization. Since the only portable OSL device
883 used for dating applications so far, the SUERC portable OSL reader, does not have an
884 internal radiation source, external sources are needed (e.g. Sanderson & Murphy, 2010;
885 Munyikwa and Brown, 2014). Secondly, for those readers that may have an internal
886 source, irradiated samples would need to be heated prior to measurement in order to
887 eliminate charges in unstable traps. However, heating a sample in a portable OSL reader
888 places challenges that would need to be overcome, ranging from excessive power
889 demand to the possibility of combustion of organics in an untreated sample, and
890 condensation of moisture from wet sediment (Roberts et al., 2018). Heating of samples
891 has been conducted outside the reader in some studies (e.g. Munyikwa and Brown,
892 2014), while other OSL readers have the means to minimize the effects of condensation
893 (e.g. Kook et al., 2011). Alternatively, samples could be dried before analyzing but that
894 may detract from the rapidity for which portable OSL readers are known. Figure 10 is an
895 SGC constructed by Munyikwa and Brown (2014) using a portable OSL reader. Test
896 doses for normalisation were applied using an external gamma-ray source. Normalized

signals were then obtained by dividing the regeneration signal (L_x) by the test dose signal (T_x) and multiplying the quotient by the test dose (T_d). In the saturation exponential used to fit the data, *I* is the standardised luminescence signal given by dose *D*, the intercept is given by I_0, and I_{max} is the upper limit for *I*. The rate at which dosimeter traps are filled determines D_0 (Munyikwa and Brown, 2014).

[Insert Figure 10]

Overall, the lack of an internal radiation source in some portable OSL readers means that the construction of SGCs as a rapid mechanism for approximating sample ages may not easily be attainable for researchers without access to an external radiation source. The lack of heating capability may also be an additional constraint to some. Nonetheless, future technical advancements in the design of portable OSL readers may render this possible. Notably, Roberts et al. (2018) have proposed three different methods for approximating D_e that do not require heating of samples and could be used with portable OSL readers. The first approach requires the derivation of a correction factor that is obtained from comparing D_e values determined using heating with those obtained using no heating. The second approach attempts to subtract the effects of the 110°C TL peak and other unstable traps from the unheated quartz signal through component fitting. The third method involves administering a small beta dose to a sample before measuring the natural signal. The beta dose fills the 110°C TL peak such that the measurement obtained

would be comparable to a regeneration measurement that has not been heated and, hence, has the same peak. While these approaches have been tested on pure quartz separates using Risø TL/OSL-DA-12 or 20 systems, they still need to be tested using bulk samples, and portable OSL readers for that matter. Thus, overall, the approaches provide scope for future development of the technique going forward.

5.2. Regression curves that compare known sample ages and their portable OSL reader signals

An approach for approximating sample ages using portable OSL reader signals that requires no irradiations nor preheating was initially introduced by Stone et al. (2015). The procedure constructed a calibration curve by plotting sample ages that had previously been determined using standard OSL protocols against luminescence signals obtained from bulk aliquots of the samples using a portable OSL reader. In the study, a total of 16 previously dated samples from the Namib Sand Sea in southern Africa, ranging in age from the last interglacial to the Late Holocene (e.g. Stone et al. 2010) were analysed using a portable OSL reader in CW mode. Importantly, dose rates, mineralogy and bleaching characteristics for the sediments were fairly uniform and burial age rather than grain size variation, variations in quartz to feldspar ratio, or sensitivity, was the main factor influencing luminescence signal intensity. A regression curve of post-IR OSL signals versus the standard OSL ages showed a good fit. To test the calibration curve, signals from samples that had been excluded in constructing the curve were used as input values

for the regression function determined on known ages samples. Results confirmed that the curve could be used to assign numerical age approximations to samples from the study area.

In a subsequent study that expanded on the earlier work, Stone et al. (2019) constructed regression curves using portable OSL signals from 144 previously dated aeolian dune samples from southern Africa. As in the earlier study, sample ages ranged from the last interglacial to the late Holocene. Apart from providing a more robust dataset, the study also investigated whether a single generic regression curve would suffice for the entire region or if region-specific curves were required. When results from individual sites were plotted to show the variation of portable reader signals and OSL ages with depth, there was good correlation between the three variables, affirming the capability of the portable OSL reader to measure relative age with depth. Plotting post-IR blue OSL signals against OSL ages for the 144 samples (Fig 11) showed that the results could be fitted into four main regional regression models. The regional groupings were largely thought to be an artifact of differences in feldspar to quartz ratio, luminescence sensitivity and local dose rates. Variations in coatings of clay or iron oxides on grains were not found to have any major effect on the signals (Stone et al., 2019).

Overall, the attractiveness of the approach by Stone et al. (2015; 2019) is that, once the calibration curve had been established, all that is required to approximate the age of a sample of unknown age is the bulk signal measured using the portable OSL reader. The modest costs associated with the procedure is such that large numbers of age estimates

966 can be obtained using minimal resources, allowing for high resolution depositional
967 frameworks to be developed. Furthermore, the rapid nature of the approach facilitates
968 effective targeting during the sample collection stage when sampling for full-fledged
969 dating (Stone et al., 2019).
970
971
972 [Insert Figure 11]
973
974
975 Similar to the method employed by Stone et al. (2015; 2019), Porat et al. (2019) calibrated
976 portable OSL reader signals to assign a numerical time scale to the geomorphic evolution
977 of archaeological terraces in the Judean Highlands of Israel. Samples were collected at
978 constant intervals from pits excavated in the terraces after which portable reader
979 measurements were made to determine post IR blue OSL signals (CW mode).
980 Additionally, samples were collected from positions that had been sampled for portable
981 reader measurements and dated using conventional OSL protocols (Figure 12a). A
982 comparison of standard OSL ages and associated portable OSL signals showed good
983 correlation, allowing a linear regression function to be derived (Figure 12b). Thus, the
984 function was used to convert the rest of the portable luminescence signals from the
985 excavation pit to numerical age approximations.
986
987
988 [Insert Figure 12]
989

While the calibration of portable OSL signals using known ages by Stone et al. (2015; 2019) examined aeolian depositional systems that were largely homogenous, the approach was extended to heterogenous depositional systems by Gray et al. (2018) who examined complex paleowetland deposits from the Las Vegas Valley in Nevada. The study aimed to ascertain if luminescence signal intensities of the interbedded aeolian and fluvial deposits had a strong age component or if the complex depositional mechanisms and provenance played a greater influence. Samples were collected from units with well-established radiocarbon and OSL ages ranging from 573 -11 ka (Gray et al., 2018) and analyzed using IRSL and blue OSL (CW mode). Regression models of the portable OSL signals against the ages showed that the data could be fitted with a quadratic equation though some scatter was observed and this possibly arose from partial bleaching in the fluvial sediment, variations in sediment source lithology, as well as differences in sensitivity. Sieving the sediment and removing magnetic minerals appeared to reduce the scatter significantly (Figure 13). Overall, the study showed that, even in complex depositional systems, age can be a major influence on paleodose levels such that burial ages can be approximated using portable OSL reader signals (Gray et al., 2018).

[Insert Figure 13]

Table 4 outlines some studies that have employed portable OSL readers to approximate sample ages. This is an area that is increasingly receiving attention and is likely to produce significant new developments in the near future.

[Insert Table 4]

6. CONCLUSION AND FURTHER OUTLOOK

Functional portable OSL readers that can be used in geomorphological applications have only been in existence for about a decade. However, a sizeable body of literature has accumulated during this period. Measurements using the instrument can be made on unprocessed samples, making the technique less resource-intensive than regular luminescence dating protocols. Additionally, the instrument can be brought closer to the field site if needed, enabling near real-time data to be obtained during fieldwork. Luminescence signal intensities of sediments are influenced by variables that include burial age, luminescence sensitivity, dose rates and mineralogy and other bulk properties. Thus, in many instances the measurements performed using the portable OSL reader allow stratigraphic features that are not visually discernible to be elucidated including cryptostratigraphic features and mixed horizons (e.g. Sanderson and Murphy, 2010). Overall, the tool can offer significant advantages when used to provide reconnaissance data as part of a luminescence dating study. The prospects of analyzing larger numbers

of samples in less time and at lower cost allows for high-resolution chronostratigraphic frameworks to be developed, which aids sample selection for conventional luminescence dating. Additionally, improved chronological insight of the stratigraphic sequences enables geomorphic contexts to be elucidated, which helps in the interpretation of the data. While studies completed to date can generally be grouped into three main categories: generation of luminescence profiles of depositional sequences, analyzing bleaching properties of sediments, and approximating ages of clastic sediments, many of the studies overlap more than one area. An overarching characteristic of the studies is that the portable OSL reader lends a rapid semi-quantitative approach to the analysis of stratigraphic sequences that would otherwise not be possible without the device.

Applications in which the portable OSL reader has been employed to date show that there is a broad range of geomorphic settings in which the instrument can be used. Clastic sediments of late Quaternary age containing either quartz or feldspar offer the best opportunities for analysis using the device. The instrument functions optimally to provide chronological information in settings where the sediment has been well bleached prior to the last burial event and where variables such as mineralogy, dose rates, and luminescence sensitivity are relatively homogenous. In more complex depositional environments, however, the utility of the portable OSL reader can be constrained as a chronostratigraphic tool, though it could be used for sediment tracing. This includes settings where dose rates vary significantly between units, or where differences exist in lithology, provenance or mineralogy such as in mixed clay sand and gravel units or in glacial and fluvial environments. Accordingly, depositional environments in which the

device has been used range from aeolian (e.g. Munyikwa et al., 2012; Bateman et al., 2015) to fluvial (e.g. Muñoz-Salinas et al., 2013; Kinnaird et al., 2015) and glacial settings (King et al., 2014). In some studies, complex sequences resulting from interactions between aeolian and fluvial (e.g. Gray et al., 2018), and marine processes have also been investigated (e.g. Palamakumbura et al., 2016; Sanderson & Kinnaird 2019) with varying degrees of success. Furthermore, the applications of the portable OSL reader span from purely geomorphological investigations (Bateman et al., 2015) to geoarchaeological and archaeological studies (e.g. Kinnaird et al., 2017; Porat et al., 2019). In essence, the utility of the instrument is multifaceted.

Apart from the widening range of applications in which the portable OSL reader have been used, the increasing body of work has notably been accompanied by greater sophistication in the type of studies being undertaken. Hopefully, going forward, this will be matched by further developments in the portable OSL reader hardware. The group at SUERC has recently introduced a double IR system that conducts stimulation using 89 nm and 940 nm wavelength sources. This setup results in ultra-high sensitivity for very young sediments which enables more recent events to be analyzed. It has also been suggested to move beyond simple profiling measurements which are largely one- or two-dimensional at best to generating three-dimensional visualizations of the chronostratigraphy (e.g. Verust et al., 2019). In particular, three-dimensional models could be advantageous for analyzing aeolian sequences that form planar bedforms, which includes many fossil dune sediments. A greater understanding of such bedforms and the associated temporal structure would be invaluable in the interpretation of luminescence

chronologies because the ages are usually obtained as point data. Three-dimensional visualization of a depositional unit would permit estimation of its magnitude, which could be related to the intensity of the environmental or climatic event during which the sediment accumulated as well as sediment supply. The spatial dimensions of the unit could also be used to infer direction of movement of an aeolian dune, which can be used to elucidate paleowind directions.

An area that has potential for growth is in the interpretation of data acquired using the portable OSL reader. To date, the interpretation of the data has largely involved univariate analysis, with only a single aspect being examined at a time. However, in many cases this is a simplification of systems that are known to be complex. Hence, it would be helpful to start incorporating portable OSL proxy variables in multivariate analyses that examine a broad range of other geomorphological variables. As indicated above, portable OSL reader signal intensities are influenced by a range of factors apart from burial age (e.g. dose rates, luminescence sensitivity, mineralogy, etc.). If these factors could be dynamically included in the analysis, the results would allow reconstructions that are cognizant of the interrelationships found in natural depositional systems. Additionally, it would make it possible to analyze geomorphic environments that are more complex.

Research in multiple other developmental areas are also in progress at the SUERC lab on topics ranging from the use of pulsed stimulation to analyze post stimulation phosphorescence and running sequences that explore time-width signal variation.

1103 However, as outlined in the introduction, these topics would be more suitable for a more
1104 dedicated review paper.
1105
1106 Finally, efforts to determine D_e using the portable reader have demonstrated the potential
1107 to expand the utility of the instrument significantly. The studies have ranged from the
1108 construction of SGCs using normalized portable OSL signals (e.g. Munyikwa and Brown,
1109 2014) to calibrating portable OSL signals using data from ages dated using standard
1110 protocols (e.g. Stone et al., 2015, 2019; Gray et al., 2018). These efforts could also benefit
1111 from the development of protocols that can be used for estimating D_e without sediment
1112 heating, as proposed by Roberts et al. (2018). If all these techniques were to be
1113 successfully refined and made functional, they would provide practitioners with a range
1114 of approaches that could routinely be used to generate approximate absolute ages using
1115 portable OSL readers, a prospect many would find invaluable. Negating sediment heating
1116 during measurement may not be useful to practitioners with portable OSL readers that
1117 do not have internal irradiators as these are required for determining D_e. However, for
1118 those with irradiators that have internal X-ray sources (e.g. the instruments developed by
1119 Takeuchi et al. (2008) and by Kook et al. (2011)), the development would certainly be
1120 consequential.
1121
1122 Overall, given the progress made to date, the application and utility of the portable OSL
1123 reader is set to expand. Its utility is gradually being affirmed by the broad diversity of
1124 geomorphic settings in which the instrument is being applied. It is possible to foresee a

time in the future when the device will be a standard tool in many studies that look at late Quaternary landscape evolution.

REFERENCES

Aitken, M.J. (1998) *An introduction to optical dating*. Oxford: Oxford University Press.

Ankjaergaard, C., Jain, M., Thomsen, K.J. and Murray, A.S. (2015) Optimising the separation of quartz and feldspar optically simulated luminescence using pulsed excitation. *Radiation Measurements*, 45, 778-785.

Bailey, R.M. (1998) Depletion of quartz OSL signal using low photon energy stimulation. *Ancient TL*, 16, 33-36.

Bateman, M.D., Rushby, G., Stein, S., Ashurst, R.A., Stevenson, D., Jones, J.M.and Gehrels, W.R. (2018) Can sand dunes be used to study historic storm events? *Earth Surface Processes and Landforms*, 43, 779-790.

Bateman, M.D., Stein, S, Ashurst, R.A. and Selby, K. (2015) Instant luminescence chronologies? High resolution luminescence profiles using a portable luminescence reader. *Quaternary Geochronology*, 30, 141-146.

Bishop, P., Muñoz-Salinas, E., Mackenzie, A.B., Pulford, I. and Mckibbin, J. (2010) The character, volume and implications of sediment impounded in mill dams in Scotland: The case of the Baldernock Mill dam in East Dunbartonshire. *Earth and Environmental Science Transactions of the Royal Society of Edinburgh*, 101, 97-110.

Brill, D., Jankaew, K. and Brückner, H. (2016) Towards increasing the spatial resolution of luminescence chronologies - Portable luminescence reader measurements and standardized growth curves applied to a beach-ridge plain (Phra Thong, Thailand). *Quaternary Geochronology*, 36, 134-147.

Brill, D., May, S.M., Shah-Hosseini, M., Rufer, D., Schmidt, C. and Engel, M. (2017) Luminescence dating of cyclone-induced washover fans at Point Lefroy (NW Australia). *Quaternary Geochronology*, 41, 134-150.

Bristow, C.S., Duller, G.A.T. and Lancaster, N. (2007) Age and dynamics of linear dunes in the Namib Desert. *Geology*, 35, 555-558.

Burbidge, C.I., Sanderson, D.C.W., Housely, R.A. and Allsworth Jones, P. (2007) Survey of Paleolithic sites by luminescence profiling: A case study from Eastern Europe. *Quaternary Geochronology*, 2, 290-302.

Carter, J, Cresswell, A.J., Kinnaird, T.C., Carmichael, L.A., Murphy, S. and Sanderson, D.C.W., 2018. Non-Poisson variations in photomultipliers and implications for

luminescence dating. Radiation Measurements, 120, 267-273. doi:10.1016/j.radmeas.2018.05.010

Castillo, M., Muñoz-Salinas, E. and Ferrari, L. (2014) Response of a landscape to tectonics using channel steepness indices (k_{sn}) and OSL: A case study from the Jalisco Block, Western Mexico. *Geomorphology*, 221, 204-214.

Clark, R.J. and Sanderson, D.C.W., (1994) Photostimulated Luminescence Excitation Spectroscopy of feldspars and micas, Radiation Measurements, 23, 641-646

Cunningham, A.C. and Wallinga, J. (2012) Realizing the potential of fluvial archives using robust OSL chronologies. *Quaternary Geochronology,* 12, 98-106.

Denby, P.M., Bøtter-Jensen, L., Murray, A.S., Thomsen, K.J. and Moska, P. (2006) Application of pulsed OSL to the separation of the luminescence components from a mixed quartz/feldspar sample. *Radiation Measurements*, 41, 774-779.

Duller, G.A.T. (2003) Distinguishing quartz and feldspar in single grain luminescence measurements. *Radiation Measurements*, 37, 161-165.

Duller G.A.T. and Bøtter-Jensen, L. (1993) Luminescence from potassium feldspars stimulated by infrared and green light. *Radiation Protection Dosimetry*, 47, 683-688.

Durcan, J.A., Roberts, H.M., Duller, G.A.T. and Alizai, A.H. (2010) Testing the use of range-finder OSL dating to inform field sampling and laboratory processing strategies. *Quaternary Geochronology*, 5, 86-90.

Galloway, R.B. (1994) Comparison of green and infrared stimulated luminescence of feldspars. *Radiation Measurements*, 23, 617-620.

Ghilardi, M., Sanderson, D., Kinnaird, T., Bicket, A., Balossino, S., Parisot, J.-C., Hermitte D., Guibal, F. and Fleury, J.T. (2015) Dating the bridge at Avignon (south France) and reconstructing the Rhone River fluvial palaeo-landscape in Provence from medieval to modern times. *Journal of Archaeological Science: Reports*, 4, 336-354.

Gray H.J., Mahan, S.A., Springer, K.B. and Pigati, J.S. (2018) Examining the relationship between portable luminescence reader measurements and depositional ages of paleowetland sediments, Las Vegas Valley, Nevada. *Quaternary Geochronology*, 48, 80-90.

Gray, H.J., Jain, M., Sawakuchi, A.O., Mahan, S.A. and Tucker, G.E. (2019) Luminescence as a Sediment Tracer and Provenance Tool. *Reviews of Geophysics*, 57, 987-1017 (https://doi.org/10.1029/2019RG000646).

Jain M. and Singhvi, A.K. (2001) Limits of depletion of blue-green light stimulated luminescence in feldspars: implication for quartz dating. *Radiation Measurements*, 33, 883-892.

Kappler, C., Kaiser, K., Tanski, P., Klos, F., Fülling, A., Mrotzek, A., Sommer, M. and Bens, O. (2018) Stratigraphy and age of colluvial deposits indicating Late Holocene soil erosion in northeastern Germany. *Catena*, 170, 224-245.

King, G.E., Sanderson, D.C.W., Robinson, R.A.J. and Finch, A.A. (2014) Understanding processes of sediment beaching in glacial settings using a portable OSL reader. *Boreas*, 43, 955-972.

Kinnaird T, Dawson T, Sanderson D. Hamilton D. Cresswell A Rennell R., (2019) Chronostratigraphy of an Eroding Complex Atlantic Round House, Baile Sear, Scotland, The Journal of Island and Coastal Archaeology, 14:1, 46-60, DOI: 10.1080/15564894.2017.1368744

Kinnaird, T., Bolos, J., Turner, A. and Turner, S. (2017) Optically-stimulated luminescence profiling and dating of historic agricultural terraces in Catalonia (Spain). *Journal of Archaeological Science*, 78, 66-77.

Kinnaird, T., Dixon, J.E., Robertson, A.H.F., Peltenburg, E. and Sanderson D.C.W. (2013) Insights on topography development in the Vasilikós and Dhiarizos Valleys,

Cyprus, from integrated OSL and Landscape Studies. Mediterranean Archaeology and *Archaeometry*, 13, 49-62.

Kinnaird, T.C., Sanderson, D.C.W. and Bigelow, G.F. (2015) Feldspar SARA IRSL dating of very low dose rate aeolian sediments from Sandwick South, Unst, Sheltand. *Quaternary Geochronology*, 30, 168-174.

Kinnaird, T.C., Sanderson, D.C.W. and Woodward, N.L. (2012) Applying luminescence methods to geoarchaeology: a case study from Stronsay, Orkney. *Earth and Environmental Science Transactions of the Royal Society of Edinburgh*, 102, 191-200.

Kocurek, G. and Ewing, R.C. (2005) Aaeolian dune field self-organization - implications for the formation of simple versus complex-dune field patterns. *Geomorphology*, 72, 94-105.

Kook, M.H., Murray, A.S., Lapp, T., Denby, P.H., Ankjaergaard, C., Thomsen., K.J., Jain, M., Choi, J.H. and Kim, G.H. (2011) A portable luminescence dating instrument. *Nuclear Instrument and Methods B*, 269, 1370 -1378.

Lichtenberger, A., Raja, R., Seland, E.H., Kinnaird, T. and Simpson, I.A. (2019) Urban-riverine hinterland synergies in semi-arid environments: millennial-scale change, adaptations, and environmental responses at Gerasa/Jerash. *Journal of Field Archaeology*, 44, 333-35.

Mills, C., Simpson I. and Adderley, P. (2014) The lead legacy: the relationship between historical mining, pollution and the post-mining landscape. *Landscape History*, 35, 47-72.

Muñoz-Salinas, E., Bishop, P., Sanderson, D.C.W., Kinnaird, T. and Zamorano, J.J. (2011) Interpreting luminescence data from a portable OSL reader: three case studies in fluvial settings. *Earth Surface Processes and Landforms*, 36, 651-660.

Muñoz-Salinas, E., Bishop, P., Sanderson, D. and Kinnaird, T. (2014) Using OSL to assess hypothesis related to the impacts of land use change with the early nineteenth century arrival of Europeans in south-eastern Australia: an exploratory case study from Grabben Gullen Creek, New South Wales. *Earth Surface Processes and Landforms*, 39, 1576-1586.

Muñoz-Salinas, E., Castillo, M., Sanderson D. and Kinnaird, T. (2013) Unravelling paraglacial activity on Sierra de Gredos, Central Spain: a study based on geomorphic markers, stratigraphy and OSL. *Catena*, 110, 207-214.

Muñoz-Salinas, E. and Castillo, M. (2018) Assessing conservation practices in Amalacaxco Gorge (Izta-Popo National Park, Central Mexico) using fallout ^{137}CS and optically stimulated luminescence (OSL). *Journal of Mountain Science*, 15, 447-460.

Muñoz-Salinas, E., Castillo, M. and Arce, J.L. (2017a) OSL signal resetting in young deposits determined with a pulsed photon-stimulated luminescence (PPSL) unit. *Boreas*, 46, 325-337.

Muñoz-Salinas, E., Castillo, M., Caballero L. and Lacan, P. (2017b) Understanding landscape dynamics of the Sierra de Juarez, southern Mexico: an exploratory approach using inherited luminescence signals. *Journal of South American Earth Sciences*, 76, 208-217.

Munyikwa, K., Brown, S. and Kitabwala, Z. (2012) Delineating stratigraphic breaks at the bases of postglacial aeolian duns in central Alberta, Canada using a portable OSL reader*. Earth Surface Processes and Landforms*, 37, 1603-1614.

Munyikwa, K. and Brown S. (2014) Rapid equivalent dose estimation for aeolian dune sands using a portable OSL reader and polymineralic standardised luminescence growth curves: expedited sample screening for OSL dating. *Quaternary Geochronology*, 22, 116-125.

Palamakumbura, R.N, Robertson, A.H.F., Kinnaird, T.C. and Sanderson D.C.W. (2016) Sedimentary development and correlation of Late Quaternary terraces in the Kyrenia Range, northern Cyprus, using a combination of sedimentology and optical luminescence data. *International Journal of Earth Sciences*, 105, 439-462.

Píšková, A., Roman, M., Bulínová, M., Pokorný, M., Sanderson, D., Cresswell, A., Lirio, J.M., Coria, S.H., Nedbalová, L., Lami, A., Musazzi, S., Van de Viyver, Nývlt D. and Kopalová, K. (2019) Late-Holocene palaeoenvironmental changes at Lake Esmeralda (Vega Island, Antarctic Peninsula) based on a multi-proxy analysis of laminated lake sediment. *Holocene*, 29, 1155-1175.

Poolton, N.R.J., Bøtter-Jensen, L, Wintle, A.G., Jakobsen, J., Jørgensen, F. and Knudsen, K.L. (1994) A portable system for the measurement of sediment OSL in the field. *Radiation Measurements*, 23, 529-532.

Porat, N., Lopez, G.I., Lensky, N., Elinson, R., Avni, Y., Elgart-Sharon, Y., Faershtein, G. and Gadot, Y. (2019) Using portable OSL reader to obtain a time scale for soil accumulation and erosion in archaeological terraces, the Judean Highlands, Israel. *Quaternary Geochronology*, 49, 65-70.

Portenga, E.W. and Bishop, P. (2016) Confirming geomorphological interpretations based on portable OSL reader data. *Earth Surface Processes and Landforms*, 41, 427-432.

Portenga, E.W., Bishop, P., Gore, D.B. and Westaway, K.E. (2016) Landscape preservation under post-European settlement alluvium in the south-eastern Australian tablelands, inferred from portable OSL reader data. *Earth Surface Processes and Landforms*, 41, 1697-1707.

Preston, J., Sanderson, D., Kinnaird, T., Newton, A., Nitter, M., Coolen, J., Mehler, N. and Dugmore, A. (2020) Dynamic beach response to changing storminess of Unst, Shetland: implications for landing places exploited by Norse communities. *Journal of Island and Coastal Archaeology,* 15, 153-178. (https://doi.org/10.1080/15564894.2018.1555193).

Rhodes, E.J. (2011) Luminescence dating of sediment over the past 200,000 years. *Annual Reviews in Earth and Planetary Sciences*, 39, 461-488.

Rittenour, T. M. (2008) Luminescence dating of fluvial deposits: applications to geomorphic, palaeoseismic and archaeological research. *Boreas*, 37, 613-635.

Roberts, H.M., Durcan, J.A. and Duller, G.A.T. (2009) Exploring procedures for the rapid assessment of optically stimulated range finder ages. *Radiation Measurements*, 44, 582-587.

Roberts, H.M., Duller, G.A.T., Gunn, M., Cousins, C.R., Cross, R.E. and Langstaff, D. (2018) Strategies for equivalent dose determination without heating, suitable for portable luminescence readers. *Radiation Measurements*, 120, 170-175.

Roberts H.M. and Wintle, A.G. (2001) Equivalent dose determinations for polymineralic fine-grains using the SAR protocol: application to a Holocene sequence of the Chinese Loess Plateau. *Quaternary Science Reviews*, 20, 859-864.

Rother, H., Lorenz, S., Börner, A., Kenzler, M., Siermann, N., Fülling, A., Hrynowiecka, A., Forler, D., Kuznetsov, V., Maksimov, F. and Starikova, A. (2019) The terrestrial Eemian to late Weichselian sediment record at Beckentin (NE-Germany): First results from lithostratigraphic, palynological and geochronological analyses. *Quaternary International*, 501, 90-108.

Sanderson, D. C. W. and Kinnaird, T. C. (2019) Optically stimulated luminescence dating as a geochronological tool for late Quaternary sediments in the Red Sea region. In: Rasul, N. M. A. and Stewart, I. C. F., (Eds.) *Geological Setting, Palaeoenvironment and Archaeology of the Red Sea*: Springer International Publishing, pp. 685-707. ISBN 9783319994079 (doi:10.1007/978-3-319-99408-6_31).

Sanderson, D.C.W. and Murphy, S. (2010) Using simple portable measurements and laboratory characterisation to help understand complex and heterogenous sediment sequences for luminescence dating. *Quaternary Geochronology*, 5, 299-305.

Sanderson, D.C.W., Bishop, P., Huston, I. and Boonsener, M. (2001) Luminescence characterization of quartz-rich cover sands from NE Thailand. *Quaternary Science Reviews*, 20, 893-900.

Sanderson, D.C.W., Bishop, P., Stark, M.T. and Spencer, J.Q. (2003) Luminescence dating of anthropologically reset canal sediments from Angkor Borei, Mekong Delta, Cambodia. *Quaternary Science Reviews*, 22, 1111-1121.

Sanderson D.C.W and Clark R.J., 1994, Pulsed Photostimulated Luminescence of Alkali Feldspars, Radiation Measurements 23, 633-639

Short, M.A. and Huntley, D.J. (1992) Infrared stimulation of quartz. *Ancient TL*, 10, 19-21.

Singhvi, A.K. and Porat, N. (2008) Impact of luminescence dating on geomorphological and paleoclimate research in drylands. *Boreas,* 37, 536-558.

Smetana, F., Hayek, M., Bergmann, M., Brusl, H., Fugger, M., Gratzl, W., Kitz, E. and Vana, N. (2008) A portable multi-purpose OSL reader for UV dosimetry at workplaces. *Radiation Measurements*, 43, 516-519.

Spooner, N.A. and Questiaux, D.G. (1989) Optical dating – Achenheim beyond the Eemian using green and infra-red stimulation. Long and short range limits in luminescence dating. *Occasional Publication* Vol 9*. The Research Laboratory for Archaeology and the History of Art, Oxford*.

Stang, D.M., Rhodes, E.J. and Heimsath, A.M. (2012) Assessing soil mixing processes and rates using a portable OSL-IRSL reader; preliminary determinations. *Quaternary Geochronology*, 10, 314-319.

Stone, A.E.C., Bateman, M.D. and Thomas, D.S.G. (2015) Rapid age assessment in the Namib Sand Sea using a portable luminescence reader. *Quaternary Geochronology*, 30, 134-140.

Stone, A., Bateman, M.D., Burrough, S.L., Garzanti, E., Limonta, M., Radeff, G. and Telfer, M.W. (2019) Using a portable luminescence reader for rapid age assessment of aeolian sediment for reconstructing dunefield landscape evolution in southern Africa. *Quaternary Geochronology*, 49, 57-64.

Takeuchi, T., Shibutani, T. and Hashimoto, T. (2008) Construction of a portable mini luminescence measurement system equipped with a miniature X-ray generator. *Geochronometria*, 30, 17-22.

Telfer, M.W. (2011) Growth by extension and reworking of a southwestern Kalahari linear dune. *Earth Surface Processes and Landforms*, 36, 1125-1135.

Thomsen, K.J., Jain, M., Murray, A.S., Denby, P.M., Roy, N. and Bøtter-Jensen, L. (2008) Minimizing feldspar OSL contamination in quartz UV-OSL using pulsed blue stimulation. *Radiation Measurements*, 43, 752-757.

Vervust, S., Kinnaird, T.C., Herring, P. and Turner, S. (2020) Dating earthworks using optically-stimulated luminescence profiling and dating (OSL-PD): the creation and development of prehistoric field boundaries at Bosigran, Cornwall (UK). *Antiquity*, 94, 420-436.

Wallinga, J., Murray, A.S. and Bøtter-Jensen, L. (2002) Measurement of the dose in quartz in the presence of feldspar contamination. *Radiation Protection Dosimetry*, 101, 367-370.

Wintle, A.G. (2008) Luminescence dating: where it has been and where it is going. *Boreas*, 37, 471-482.

ACKNOWLEDGEMENTS

Susan Fryters is thanked for proofreading several versions of this manuscript.

FIGURE CAPTIONS

Figure 1 (a) The third-generation SUERC portable luminescence reader. (b) The instrument weighs less than 5 kg and can be transported in a briefcase-sized holder.

Figure 2 Typical luminescence signal curves obtained using the SUERC portable OSL reader. (a) IRSL and post-IR blue OSL shine-down curves obtained following stimulation of a bulk sample of aeolian sands from central Alberta for 120 seconds. (b) Same sample stimulated for 120 seconds using a pulsed signal (15 μs up and 15 μs down). In both cases, dark count periods of 10 s before and after stimulation were used.

Figure 3 Illustration of IRSL and blue OSL signals measured using the portable OSL reader that increase gradually with depth (and age) in a depositional sequence. (a) IRSL and blue OSL signals measured on samples from an aeolian dune in central Alberta, Canada. (Adapted from Munyikwa et al., 2012). (b) signals from fluvial deposits (sand and silty clay) from Grabben Gullen Creek in SE Australia. (Adapted from Portenga et al., 2016).

Figure 4 Luminescence signals from a coastal aeolian dune sequence in Norfolk County, UK deposited over a relatively short period of time. The entire profile accumulated over a ca. 15 year period. (Adapted from Bateman et al., 2015).

Figure 5 IRSL and post-IR blue OSL profiles showing inverted signal distribution. (a) Signals from a Neolithilic ditch exposed in a quarry section at Cava Petrilli, Italy. The stratigraphy shows a darker lower ditch fill, possibly an agricultural soil overlain by an upper fill comprising post-abandonment backfill derived from poorly bleached former substrate material (Adapted from Sanderson and Murphy, 2010). (b) Signals from fluvial sediment from Grabben Gullen Creek, southeast Australia. Poorly bleached post-settlement alluvium (PSA) overlies swampy meadow (SM) alluvium that was well bleached at deposition (Adapted from Muñoz-Salinas et al., 2014).

Figure 6 IRSL and OSL profiles depicting an interface between units of different age. (a) Signals from an abandoned fluvial channel in Cambodia. Units I/II were radiocarbon dated as modern while organic material from III/IV returned an age of ca. 6 ka (Adapted from Muñoz-Salinas et al., 2011). (b) A profile and signals from aeolian sands (unit 6) aged about 14 ka overlying last Interglacial lake sediment (ca 114-118 ka) from Beckentin , NE Germany (Adapted from Rother et al., 2019).

Figure 7 The variation of IRSL and post-IR signal intensities with distance from the ice margin recorded from braid-bar and side-attached bar deposits at Bergsetdalen, Jostedalen, southern Norway. Overall, signals are higher and the scatter in signals greater closer to source than further downstream (Adapted from King et al., 2014).

Figure 8 The variation of IRSL ‘effective ages’ with depth for three different monoliths sampled in the San Gabriel Mountains, California. Note that the ‘effective ages’ do not

equal depositional ages of the sediments since the ages were obtained from mixed grain populations. (a) For Monolith A, two episodes during which the sediment may have been at the surface are shown. (b) For Monolith B, the high degree of fluctuation in 'effective age' was thought to indicate a high soil turnover history, possibly resulting from extensive bioturbation. (c) For Monolith C, the constant signals in the upper part of the soil profile suggested the presence of a soil macropore that was filled by surface sediment during a storm or slumping event (Adapted from Stang et al., 2012).

Figure 9 Variation in IRSL signals with distance downstream along ravines in (a) areas under conservation and (b) areas under natural vegetation. In areas under conservation, signals increase downstream because the stream entrains poorly bleached samples with distance. In areas under natural vegetation, sediment is only sourced upstream and it bleaches with distance (Adapted from Munoz-Salinas et al., 2018).

Figure 10 SGC constructed by Munyikwa and Brown (2014) for central Alberta using portable OSL reader measurements. Samples used to construct the curve were collected from six different sites. To approximate D_e for a sample of unknown age, a sample's natural signal is measured using the portable OSL reader after which a test dose is applied (gamma ray) to normalize the natural signal. Interpolating the normalized signal into SGC provides the required D_e value (Adapted from Munyikwa and Brown, 2014).

Figure 11 Regression models of southern African aeolian dune sample OSL ages plotted against portable OSL reader bulk post-IR blue OSL signals. Four main regional curves were obtained (Adapted from Stone et al., 2019).

Figure 12 (a) A plot of luminescence signal versus depth in a pit excavated in an agricultural terrace in the Judean Highlands of Israel . Also shown are sampling positions of samples dated using standard OSL protocols. (b) A regression model of sample age versus blue OSL signal. The derived function was then used to calculate ages of samples of unknown age whose signals are indicated in Figure 12(a) (Adapted from Porat et al., 2019).

Figure 13 Quadratic curve derived from portable OSL reader signals plotted against ages established using radiocarbon and standard OSL procedures. Data shown above are after sieving and removal of magnetic minerals using hand magnet (Adapted from Gray et al., 2018).

1530 **TABLE 1** Summary of major positive features and drawbacks of portable OSL readers examined in this
1531 paper
1532

Portable OSL Reader developed by:	Major Positive Attributes	Potential Limitations
Poolton et al. (1994)	• Lightweight (<5kg). • Sample cartridge can hold up to 12 samples. • Hg discharge lamp for signal normalisation. • Dedicated sample bleaching lamp (blue). • CW sample stimulation mode	• Primarily targets feldspar for analysis (source for quartz stimulations can be added). • No pulsed stimulation. • No irradiation source. • Instrument never developed past prototype version. • Requires 12V DC power source.
Takeuchi et al. (2008)	• Sample cartridge can hold up to 13 samples. • RTL and OSL measurement possible. • Has both IR stimulation source (for feldspar) and blue light (for quartz). • Performs both CW and pulsed-OSL sample stimulation (can gate photon counting during pulsed-OSL). • Sample heating possible (up to 600° C) • X-ray generator for artificial irradiation. • Can operate on 5V DC power source (when heating not required).	• Weighs about 15 kg • Instrument never developed past prototype version.
SUERC (Sanderson and Murphy, 2010)	• Lightweight (<5kg). • Has both IR stimulation source (for feldspar) and blue light (for quartz). • Simple and robust operation. • Instrument used in multiple studies in a wide range of environments. • Performs CW and pulsed-OSL sample stimulation. • Can operate on 5V DC power source.	• No irradiation source. • Sample tray only holds one sample at a time. • No heating element • Cannot gate photon counting during pulsed-OSL.
Kook et al. (2011)	• Lightweight (about 5 kg). • X-ray generator for artificial irradiation. • Performs both CW and pulsed-OSL sample stimulation (can gate photon counting during pulsed-OSL). • Has IR and blue LED sources for sample bleaching. • Sampler doubles as sample holder during measurement (prevents sample exposure to light when sampling). • Sample heating possible (up to >250° C) • Can operate on 9V DC power source.	• Primarily targets quartz for analysis (no IRSL sources for measurement.) • Power requirement up to 45 V DC when heating required. • Samples with organic material may be difficult to heat.

1533

1534

1535

1536 **TABLE 2** Studies that have conducted luminescence profiling using a portable luminescence reader
1537

Environment	References and Study Region	Application
Fluvial / Colluvial	Muñoz-Salinas et al., 2011 (Cambodia); Kinnaird et al., 2013 (SW Cyprus); Muñoz-Salinas et al., 2014 (SE Australia); Palamakumbura et al., 2016 (N Cyprus); Portenga and Bishop, 2016 (SE Australia); Portenga et al., 2016 (SE Australia); Kappler, et al, 2018 (NE Germany); Lichtenberger et al., 2019 (Jordan).	OSL profiling used to identify boundaries between units of different age (unconformities) or units with different signals resulting from different mineralogies (e.g. quartz to feldspar ratio). Different signals may also be an artifact of provenance. Signals may provide information on transport mechanisms. Enables the screening of sediment suitable for OSL dating.
Coastal	Sanderson and Murphy, 2010 (Thailand); Kinnaird et al., 2012 (Orkney, UK); Bateman et al., 2015 (Norfolk, UK); Kinnaird et al., 2015 (Shetland Islands, UK); Brill et al., 2017 (NW Australia); Preston et al., 2020 (Shetland, UK).	OSL profiling used to identify interfaces between units of different age or between well-bleached and poorly bleached sediments (e.g. Tsunami-wave deposits atop onshore deposits). Luminescence signals provide information on possible transport mechanisms. Enables the selection of sediment appropriate for dating.
Archaeological	Sanderson and Murphy, 2010 (Italy); Ghilard et al., 2015 (Avignon, France); Kinnaird et al. 2017 (Catalonia, Spain); Porat et al., 2019 (Israel); Lichtenberger et al., 2019 (Jordan); Vervust, et al., 2019 (Cornwall, UK).	Examined features include ditch fills, earthworks, historical bridge construction, mine workings and agricultural terraces. Profiling used to identify depositional units of different age and to distinguish priority targets for dating using OSL methods.
Aeolian (inland)	Munyikwa et al., 2012 (AB, Canada); Rother et al., 2019 (NW Germany)	OSL profiling used to differentiate between units that were bleached well prior to burial and those that were not. Profiling also used to identify interfaces between depositional units of different age (unconformities).
Glaciolacustrine	Píšková et al., 2019 (Vega Island, Antarctic Peninsula)	OSL profiling conducted on lake sediment cores to identify samples for dating using regular OSL methods.
Offshore/marine	Sanderson and Kinnaird, 2019 (Red Sea)	OSL profiling of marine cores allowed the identification Pleistocene units, beneath more recent Holocene sediments on the continental shelf of the Red Sea near the Farasan Islands
Paraglacial	Muñoz-Salinas et al., 2013 (Sierra de Gredos, Spain)	Profiling of debris flows and fluvial deposits in paraglacial landscapes to obtain relative chronology of deposition prior to sampling for OSL dating.

1538
1539
1540
1541
1542
1543
1544
1545

1546 **TABLE 3** Studies that have employed portable OSL readers to explore sediment bleaching
1547

Environment	References and Study Region	Applications
Pedogenic / soils	Stang et al., 2012 (California, USA)	OSL reader signals used to study patterns and rates of soil mixing. Results suggest that there are multiple processes that are operating to result in vertical movement of mineral grains in soils, including bioturbation and filling of macropore by sediment during storm or slump events. Findings allow soil turnover history to be calculated.
Glaciofluvial	King et al., 2014 (Jostdalen, Norway)	Modern glacial sediments analyzed in an effort to gain insight into catchment-scale sediment bleaching processes. Results show that high-magnitude processes of low frequency are characterized by poor sediment bleaching whereas low-magnitude events that occur with higher frequency are associated with best chances for sediment bleaching.
Orogenic /tectonic uplift	Castillo et al., 2014 (Western Mexico)	Portable OSL reader measurements used to investigate rates of erosion in the Jalisco Block in order to assess geomorphic response to differential uplift. Results showed that higher uplift rates in the northern sector produces higher relief that corresponds with more turbid flows such that sediments in riverbeds are poorly bleached.
Volcanic /coastal / fluvial	Muñoz-Salinas et al., 2017a (Mexico)	Portable OSL reader used to examine young sediments (<2ka) from volcanic, coastal and fluvial environments in order to differentiate between sediments that are most effectively zeroed from those that are poorly bleached. Findings indicate that debris flow sediments are most likely to be poorly bleached. IRSL signals of volcanic ash, lavas, and sand beach and dune deposits show minimal scatter whereas blue OSL signals display significant scatter, likely due to charge transfer or low quartz sensitivity.
Fluvial	Muñoz-Salinas et al., 2017b (Oaxaca, Mexico); Muñoz-Salinas and Castillo, 2018 (Izta-Popo, Mexico)	Residual IRSL and blue OSL signals in fluvial sediments were investigated using a portable OSL reader to gain insight into mechanisms involved during debris flows. Results suggest sediment grains are transported without stratification; deposits from steeper channels have higher signals as a result of more turbid flows. Another study compared degree of bleaching in sediment in natural areas to that in areas under conservation. Results show that sediment in ravines that cut into natural forest and alpine grassland are better bleached than sediment in alpine grassland under conservation practice. Hence, curbing the effects of human activity in the area appears to be ineffective.
	Lichtenberger et al., 2019 (Wadi Suf, Jordan)	Portable OSL reader used to examine sediment in three sections along Wadi Suf in a study looking at the relationship between urban settlement and riverine systems in semi-arid environments. Results show that both IRSL and blue OSL signal intensities increased downstream suggesting increase in sensitivity due to repeated erosion-deposition cycles.

1548
1549
1550
1551
1552
1553
1554

1555 **TABLE 4** Select studies that have employed portable OSL readers to approximate sample age
1556

Environment	References and Study Region	Methodology
Aeolian (inland)	Munyikwa and Brown, 2014 (AB, Canada)	SGC was constructed using regeneration method (Figure 6); signals were normalized using a gamma source (^{137}Cs). SGC showed linear growth up to at least 100 Gy. D_es of natural samples of unknown ages were determined by acquiring a portable OSL reader signal of bulk sample and normalizing it and then comparing with SGC for corresponding D_e. Large uncertainties but results generally show capacity to approximate D_e for samples within region.
Aeolian (inland)	Stone et al., 2015 (Namib Sand Sea, Namibia)	Study aimed to convert portable OSL readings into luminescence age estimates. Samples whose ages have been determined using standard luminescence dating protocols were measured using a portable OSL reader. Acquired signals were plotted against sample age to produce a regional calibration curve (linear regression) for rapid age approximation. Resulting calibration curve tested by measuring portable signals for samples whose ages are known but were not used to construct the curve. Predicted sample ages consistent with the real ages.
Coastal	Brill et al., 2016 (Phra, Thong, Thailand)	Study conducted using both luminescence profiling and SGCs of samples whose ages had previously been dated using standard luminescence dating protocols. SGC constructed using bulk samples and a regular Risø TL-DA system. The broad depositional chronology ranging from late Holocene to last interglacial can be elucidated by the SGC data. However, the ages have large uncertainties, making it difficult to identify shorter events.
Wetlands	Gray et al., 2018 (Las Vegas Valley, Nevada, USA)	Study analyzed the relationship between portable OSL reader signals of paleowetland deposits of middle to late Pleistocene age and their absolute ages that had been determined using standard luminescence dating protocols to see if portable OSL reader signals can reliably be used to predict sample ages at the site. Sediment sources are thought to be aeolian and fluvial. Plots of sample age versus IRSL/OSL signals fitted with a quadratic equation. Despite significant scatter, results indicate that portable OSL reader signals correlate with sample age.
Aeolian	Stone et al., 2015, 2019 (Namib Sand Sea, Namibia).	Study builds on work by Stone et al. (2015) by using a larger set of samples. Portable OSL reader signals of 144 aeolian samples from four regions in southern Africa whose ages have been established using regular luminescence dating protocols were acquired. A regression analysis of the signals versus established age of samples shows that there are region-specific relationships between sample age and signals that can be used to predict approximate ages of samples of unknown age. Overall, the data suggest that the large number of samples used in the regression curve improve the quality of the results. Results were tested statistically using coefficient of determination and root mean square error. Findings indicate that there is a strong correlation between portable OSL reader signals and sample age, and regression curves can be used to predict ages reliably.
Coastal	Kinnaird et al., 2019 (Bile Sear, Scotland)	A series of portable OSL sequences (>58) were expressed as apparent ages by cross calibration to full OSL dating samples. Bayesian sequences of the interdigitated chronologies of both the OSL dates, and the larger number of profiling apparent ages were developed and used to generalise the chronostratigraphy of the site.

1557
1558

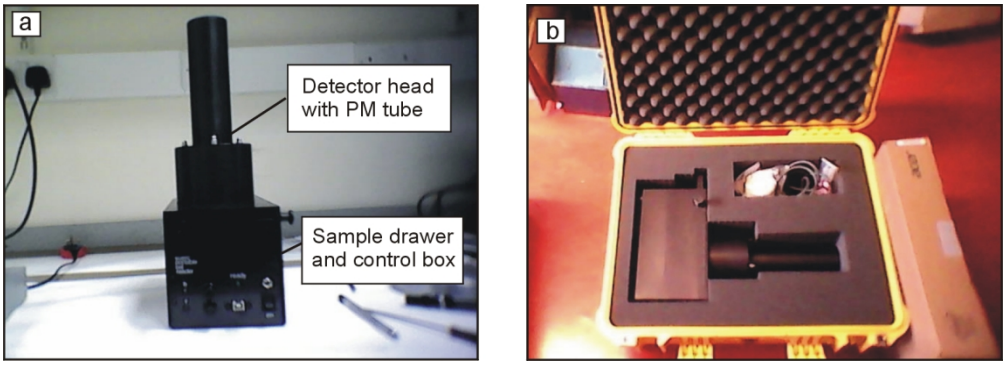

Figure 1 (a) The third-generation SUERC portable luminescence reader. (b) The instrument weighs less than 5 kg and can be transported in a briefcase-sized holder.

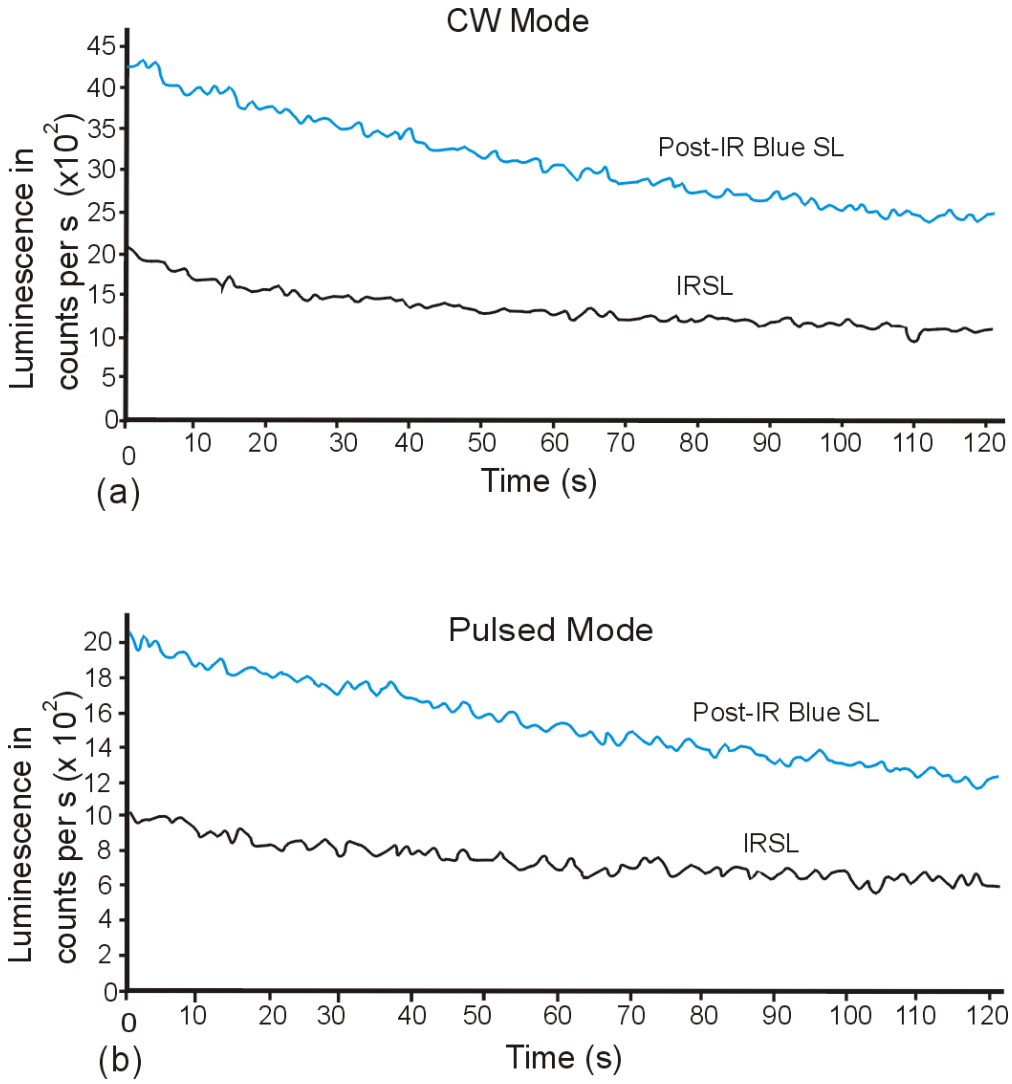

Figure 2 Typical luminescence signal curves obtained using the SUERC portable OSL reader. (a) IRSL and post-IR blue OSL shine-down curves obtained following stimulation of a bulk sample of aeolian sands from central Alberta for 120 seconds. (b) Same sample stimulated for 120 seconds using a pulsed signal (15 μs up and 15 μs down). In both cases, dark count periods of 10 s before and after stimulation were used.

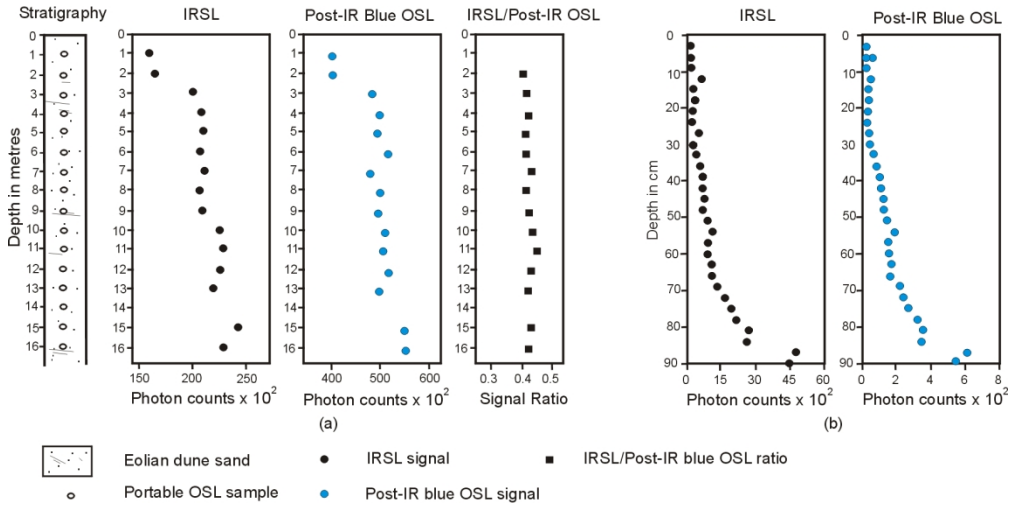

Figure 3 Illustration of IRSL and blue OSL signals measured using the portable OSL reader that increase gradually with depth (and age) in a depositional sequence. (a) IRSL and blue OSL signals measured on samples from an aeolian dune in central Alberta, Canada (Adapted from Munyikwa et al., 2012). (b) signals from fluvial deposits (sand and silty clay) from Grabben Gullen Creek in SE Australia (Adapted from Portenga et al., 2016).

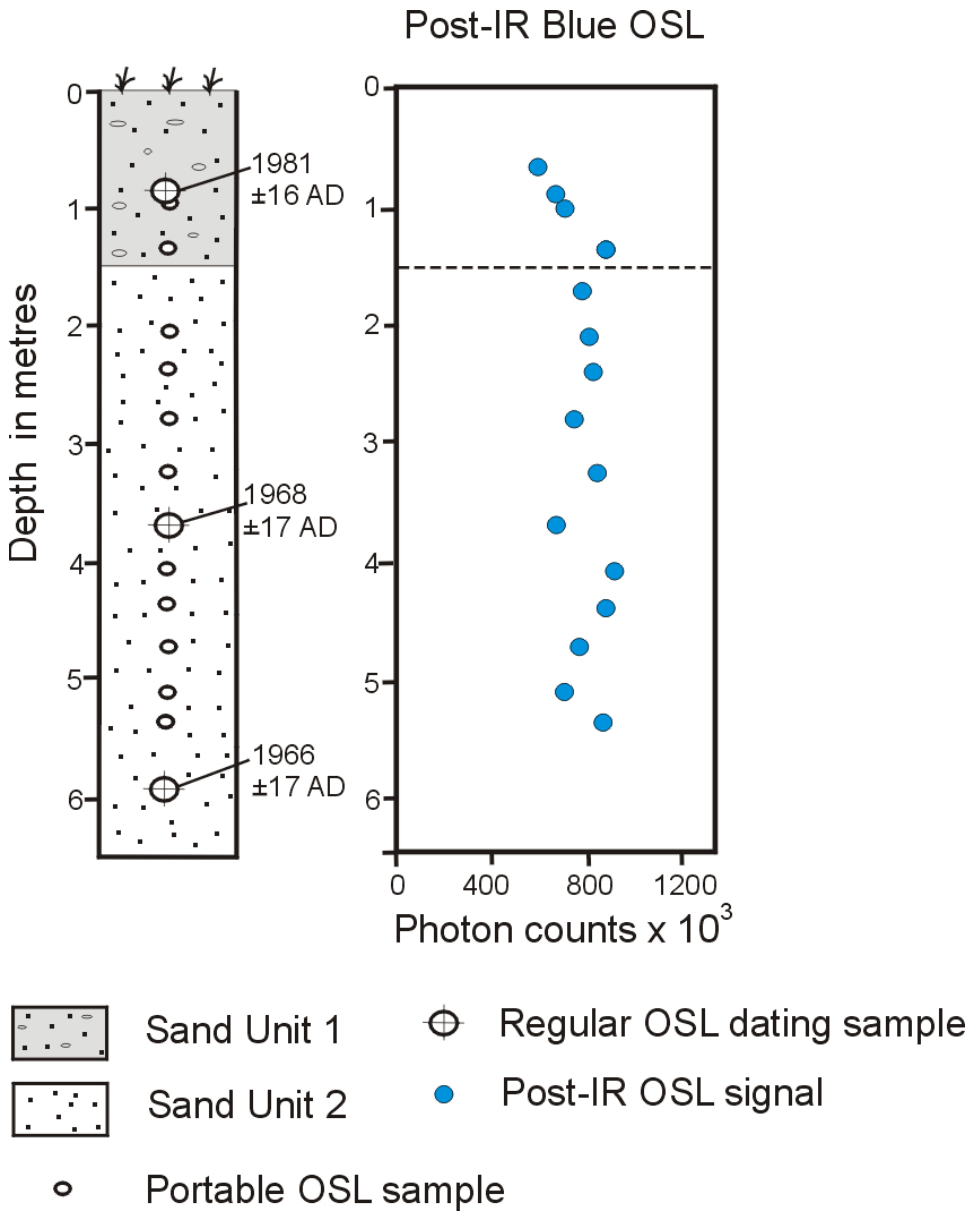

Figure 4 Luminescence signals from a coastal aeolian dune sequence in Norfolk County, UK deposited over a relatively short period of time. The entire profile accumulated over a ca. 15 year period (Adapted from Bateman et al., 2015).

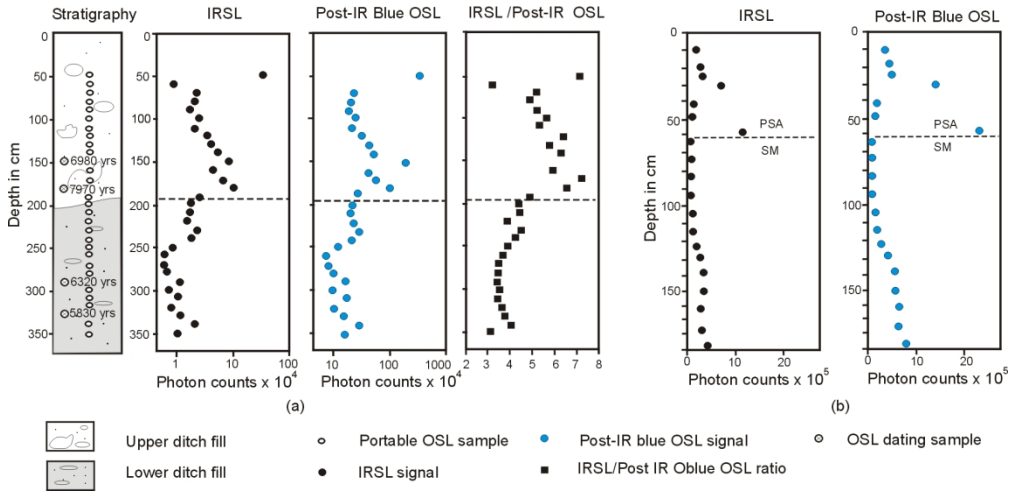

Figure 5 IRSL and post-IR blue OSL profiles showing inverted signal distribution. (a) Signals from a Neolithilic ditch exposed in a quarry section at Cava Petrilli, Italy. The stratigraphy shows a darker lower ditch fill, possibly an agricultural soil overlain by an upper fill comprising post-abandonment backfill derived from poorly bleached former substrate material (Adapted from Sanderson and Murphy, 2010). (b) Signals from fluvial sediment from Grabben Gullen Creek, southeast Australia. Poorly bleached post-settlement alluvium (PSA) overlies swampy meadow (SM) alluvium that was well bleached at deposition (Adapted from Muñoz-Salinas et al., 2014).

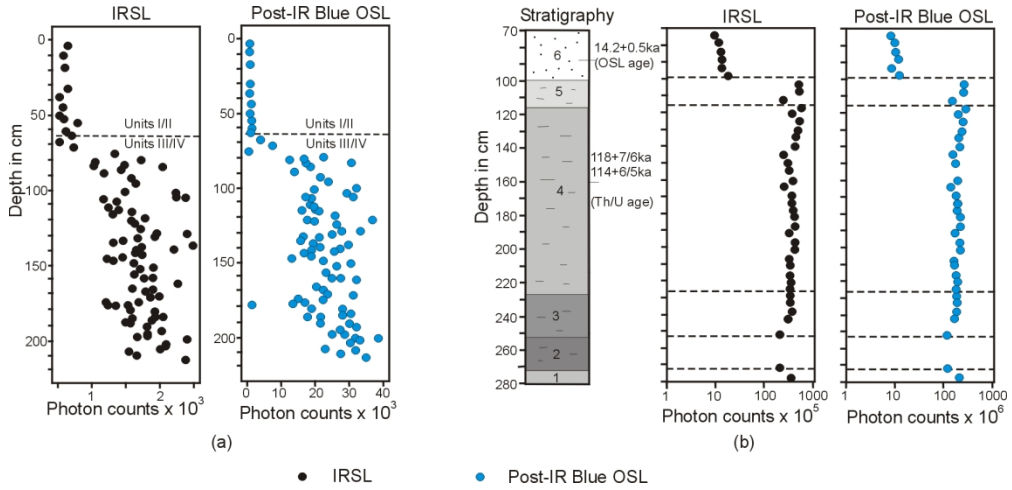

Figure 6 IRSL and OSL profiles depicting an interface between units of different age. (a) Signals from an abandoned fluvial channel in Cambodia. Units I/II were radiocarbon dated as modern while organic material from III/IV returned an age of ca, 6 ka (Adapted from Muñoz-Salinas et al., 2011). (b) A profile and signals from aeolian sands (unit 6) aged about 14 ka overlying last Interglacial lake sediment (ca 114-118 ka) from Beckentin , NE Germany (Adapted from Rother et al., 2019).

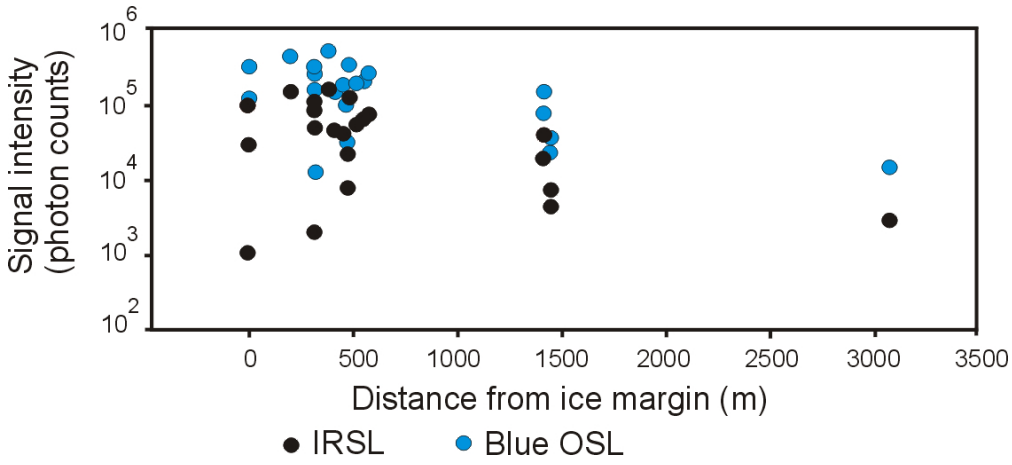

Figure 7 The variation of IRSL and post-IR signal intensities with distance from the ice margin recorded from braid-bar and side-attached bar deposits at Bergsetdalen, Jostedalen, southern Norway. Overall, signals are higher and the scatter in signals greater closer to source than further downstream (Adapted from King et al., 2014).

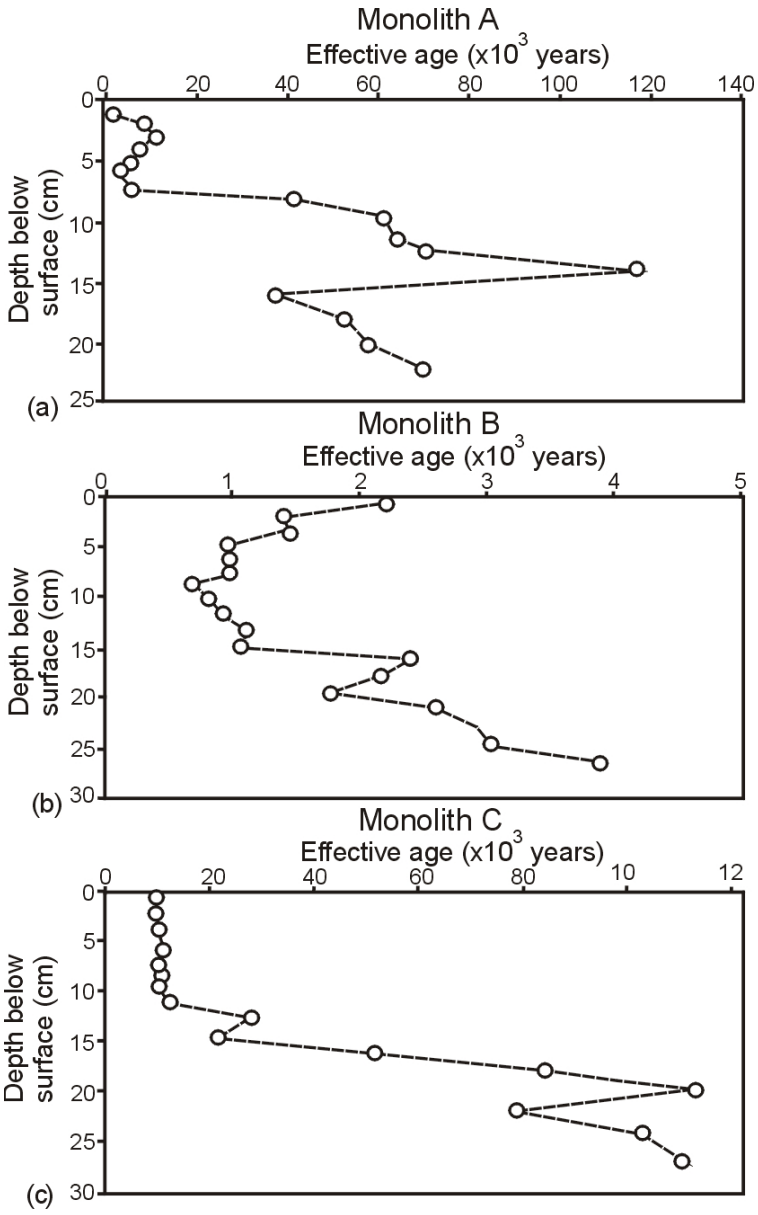

Figure 8 The variation of IRSL 'effective ages' with depth for three different monoliths sampled in the San Gabriel Mountains, California. Note that the 'effective ages' do not equal depositional ages of the sediments since the ages were obtained from mixed grain populations. (a) For Monolith A, two episodes during which the sediment may have been at the surface are shown. (b) For Monolith B, the high degree of fluctuation in 'effective age' was thought to indicate a high soil turnover history, possibly resulting from extensive bioturbation. (c) For Monolith C, the constant signals in the upper part of the soil profile suggested the presence of a soil macropore that was filled by surface sediment during a storm or slumping event (Adapted from Stang et al., 2012).

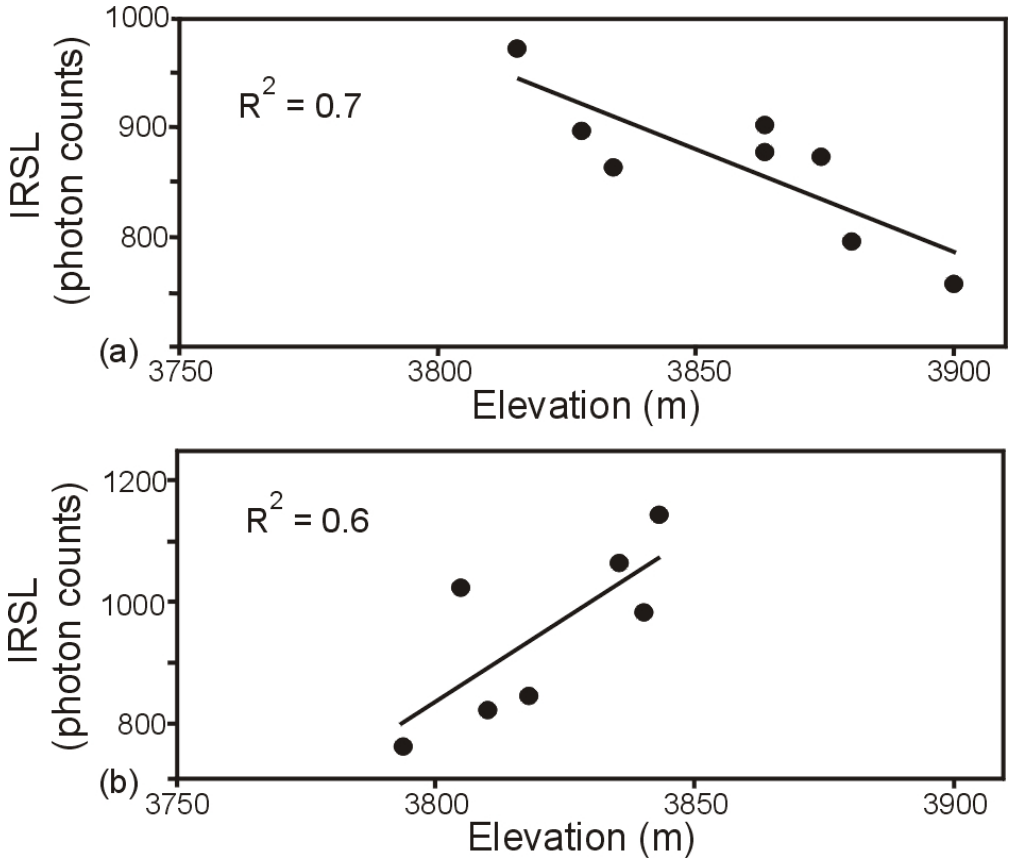

Figure 9 Variation in IRSL signals with distance downstream along ravines in (a) areas under conservation and (b) areas under natural vegetation. In areas under conservation, signals increase downstream because the stream entrains poorly bleached samples with distance. In areas under natural vegetation, sediment is only sourced upstream and it bleaches with distance (Adapted from Munoz-Salinas et al., 2018).

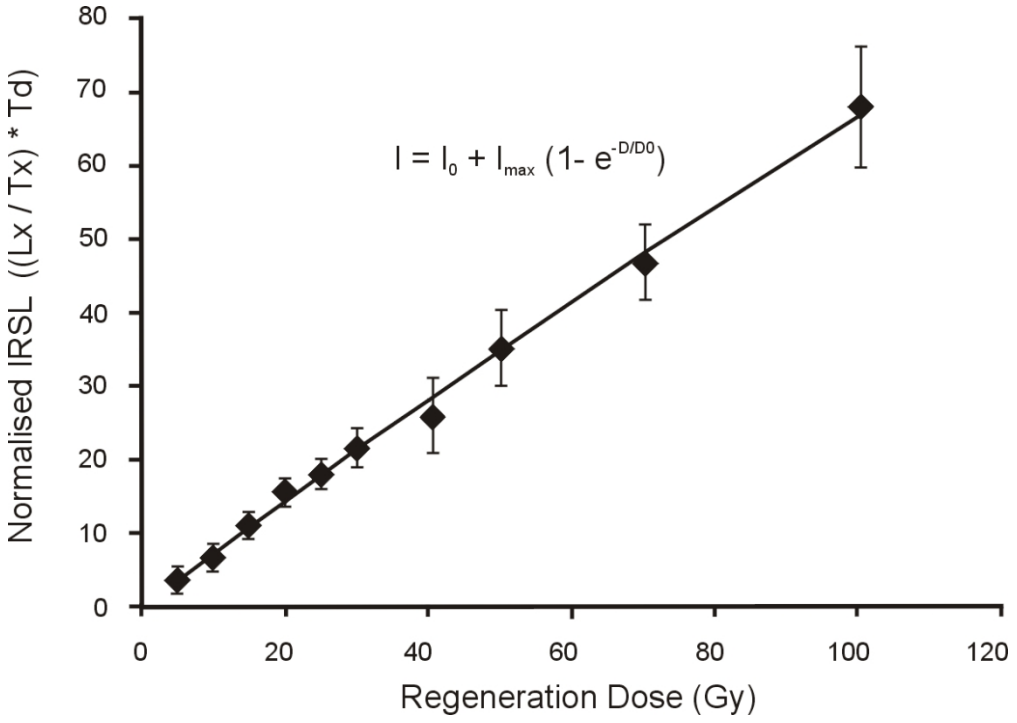

Figure 10 SGC constructed by Munyikwa and Brown (2014) for central Alberta using portable OSL reader measurements. Samples used to construct the curve were collected from six different sites. To approximate the equivalent dose (De) of a sample of unknown age, a sample's natural signal is measured using the portable OSL reader after which a test dose is applied (gamma ray) to normalize the natural signal. Interpolating the normalized signal into SGC provides the required De value (Adapted from Munyikwa and Brown, 2014).

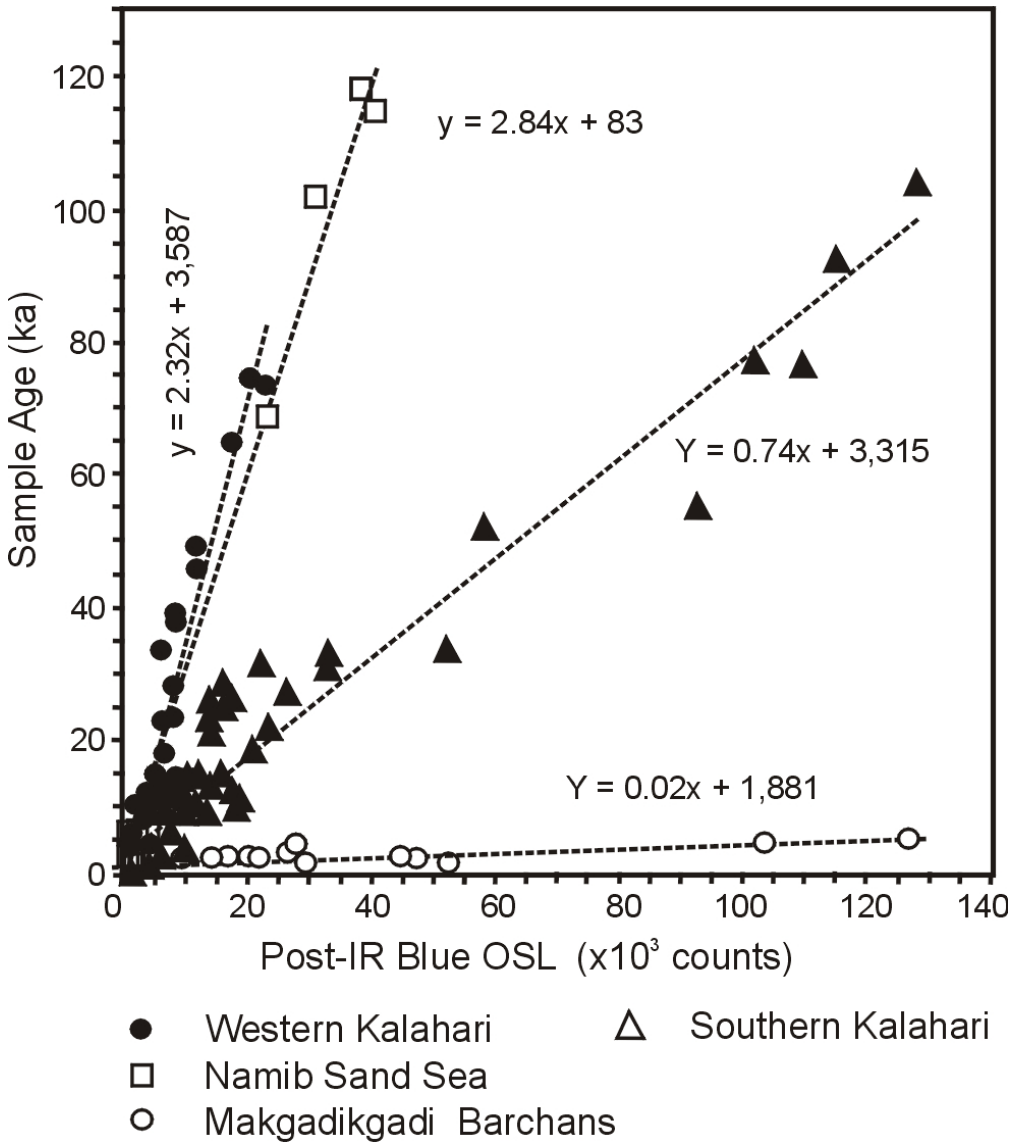

Figure 11 Regression models of southern African aeolian dune sample OSL ages plotted against portable OSL reader bulk post-IR blue OSL signals. Four main regional curves were obtained (Adapted from Stone et al., 2019).

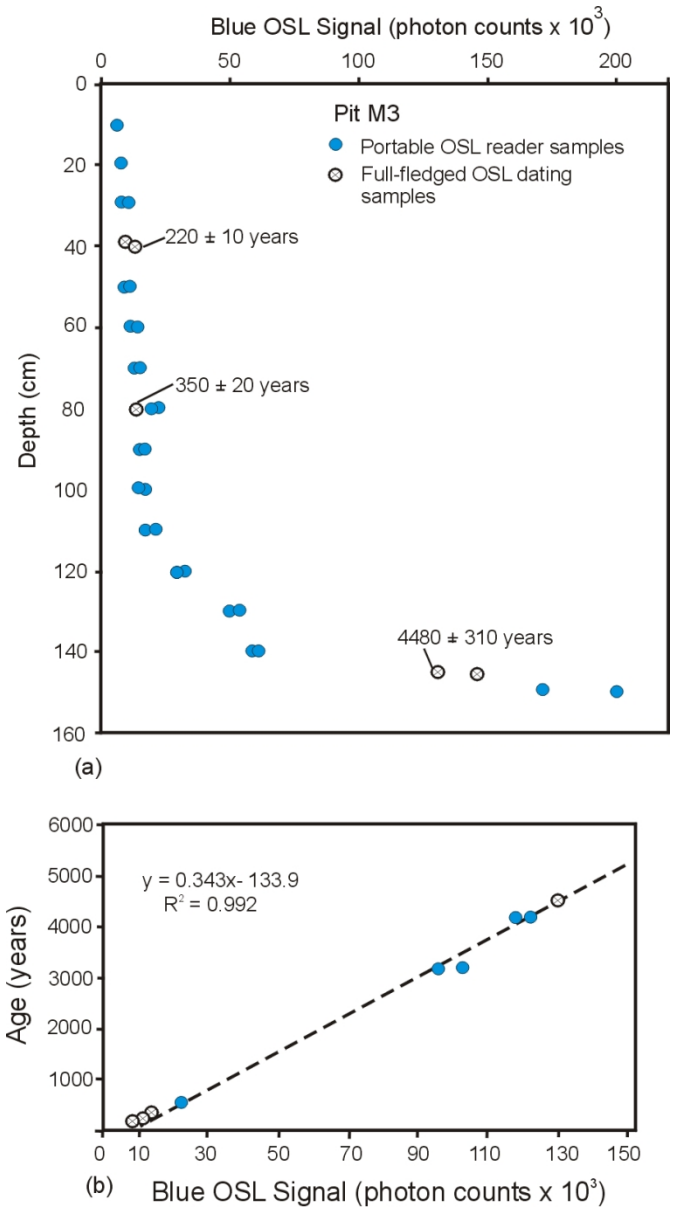

Figure 12 (a) A plot of luminescence signal versus depth in a pit excavated in an agricultural terrace in the Judean Highlands of Israel . Also shown are sampling positions of samples dated using standard OSL protocols. (b) A regression model of sample age versus blue OSL signal. The derived function was then used to calculate ages of samples of unknown age whose signals are indicated in Figure 12(a) (Adapted from Porat et al., 2019).

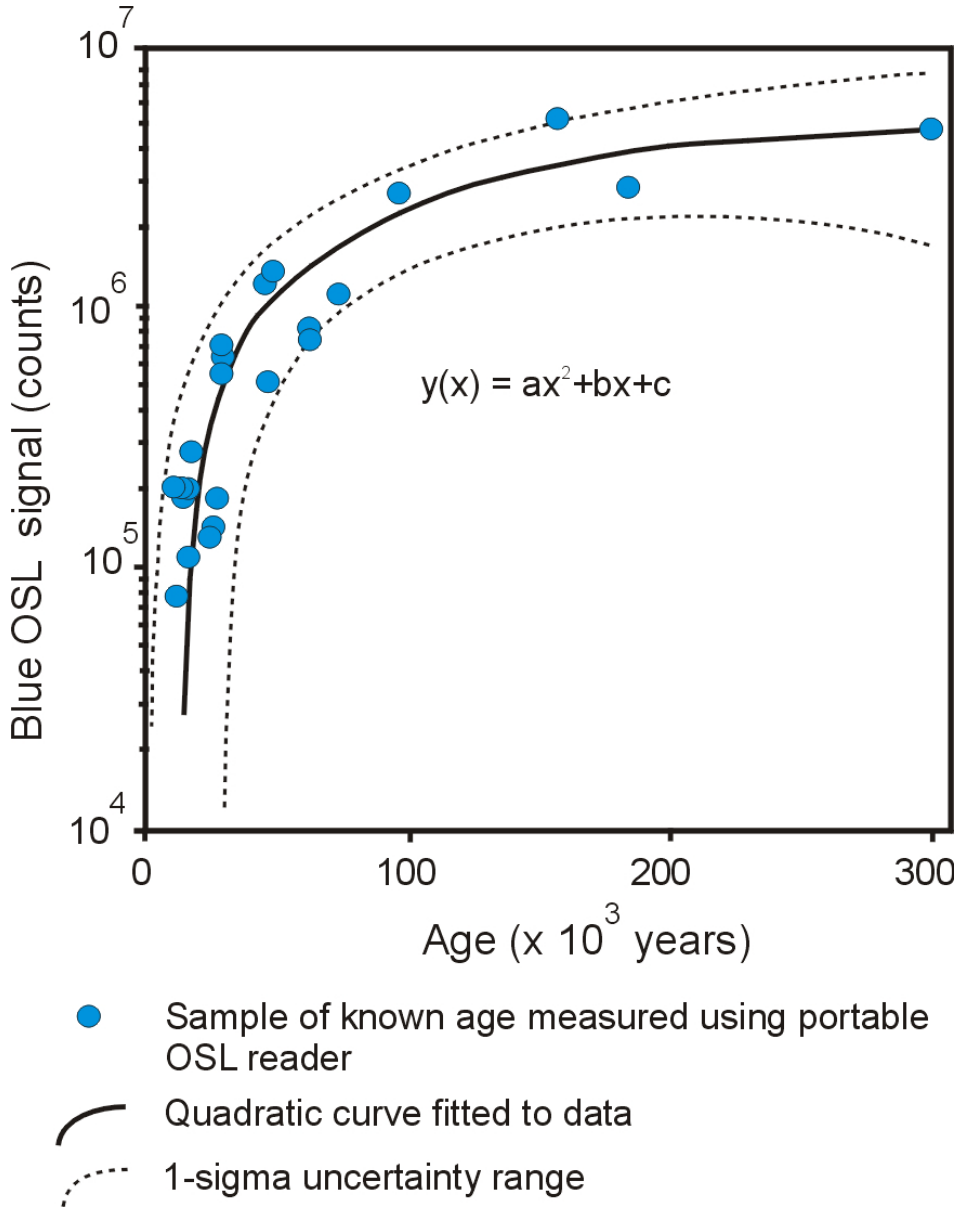

Figure 13 Quadratic curve derived from portable OSL reader signals plotted against ages established using radiocarbon and standard OSL procedures. Data shown above are after sieving and removal of magnetic minerals using hand magnet (Adapted from Gray et al., 2018).